Rev Environ Sci Biotechnol (2020) 19:149–190
https://doi.org/10.1007/s11157-020-09526-0

REVIEW PAPER

Recent developments in textile wastewater biotreatment: dye metabolite fate, aerobic granular sludge systems and engineered nanoparticles

Rita Dias Guardão Franca · Helena Maria Pinheiro · Nídia Dana Lourenço

Published online: 14 February 2020

Abstract Textile wastewater (TWW) represents a major source of pollution worldwide, carrying high organic loads, recalcitrant azo dyes and engineered nanoparticles (ENP), namely silver nanoparticles (AgNP). The development of cost-efficient, environmentally-friendly TWW treatment solutions is critical. Despite the successful biodecolorization of azo dyes under anaerobic conditions, clear evidence for subsequent aerobic biodegradation of the often toxic breakdown sulfonated aromatic amines is scarce. Moreover, the debatable AgNP toxicity mechanisms, and apparent AgNP retention in activated sludge have raised concerns regarding eventual negative impacts on wastewater treatment efficiency. The aerobic granular sludge (AGS) technology, which has recently been scaled-up and implemented for the treatment of domestic wastewater and some industrial wastewaters, seems highly promising for TWW treatment, due to the high biomass retention capacity, anaerobic/anoxic/aerobic microenvironments within granules and enhanced tolerance towards high organic loads and toxic compounds. A review of the existing literature on AGS application to TWW treatment is presented, with a focus on the removal of azo dyes and their metabolites and ENP. The applicability of AGS to dye-containing synthetic and real TWW has been tested in different SBR systems. Their hydrodynamic regimens and operational conditions have been optimized, namely regarding granulation, long-term stability, azo dye decolorization and biodegradation of aromatic amines. Although promising results have been published regarding AGS resistance towards ENP (particularly AgNP), their long-term effects on the physical stability, biochemical properties and microbial community of AGS deserve more investigation. Overall, this review provides relevant support for the application of AGS SBRs in TWW treatment as a potential sustainable alternative to avoid the pollution of natural water bodies with synthetic dyes and ENP.

Keywords Aerobic granular sludge · Aromatic amine biodegradation · Azo dye biodegradation · Sequencing batch reactors · Silver nanoparticles · Textile wastewater treatment

R. D. G. Franca · H. M. Pinheiro · N. D. Lourenço
iBB – Institute for Bioengineering and Biosciences, Department of Bioengineering, Instituto Superior Técnico, Universidade de Lisboa, Av. Rovisco Pais, 1049-001 Lisbon, Portugal

N. D. Lourenço (✉)
UCIBIO-REQUIMTE, Department of Chemistry, Faculty of Sciences and Technology, Universidade NOVA de Lisboa, 2829-516 Caparica, Portugal
e-mail: nidia.lourenco@fct.unl.pt

1 Introduction

Owing to the increasing demand for textile products by a growing population, the textile industry production and its pollutant wastewaters have been increasing proportionally, making it one of the most chemically intensive industries on Earth and, possibly, the main industrial consumer and polluter of potable water worldwide (Dasgupta et al. 2015; Holkar et al. 2016; Nimkar 2018; Vajnhandl and Valh 2014). The textile industry generates large amounts of wastewater with a complex mixture of chemicals and extremely variable characteristics (Vajnhandl and Valh 2014; Verma et al. 2012). As a consequence of discharging a significant amount of the chemicals employed along the textile processing, TWWs are generally characterized by high organic loads and salinity, as well as low biodegradability, especially due to recalcitrant dyes (Dasgupta et al. 2015; dos Santos et al. 2007; Sarayu and Sandhya 2012).

Direct discharge of untreated or poorly treated TWWs into surface waters can affect fauna, flora and microbial communities. Specifically, the high organic and nutrient loads typically associated with these effluents can promote the overgrowth of aquatic flora and consequent depletion of dissolved oxygen (DO), ultimately leading to eutrophication of the water body (Sarayu and Sandhya 2012). Furthermore, the presence of color and suspended solids can inhibit the photosynthetic processes by decreasing sunlight penetration in water, thus disturbing the ecological balance (Collivignarelli et al. 2019; Pandey et al. 2007). In addition, some chemicals found in TWWs can be acutely toxic to aquatic life (Ghaly et al. 2014).

The development of efficient, environmentally friendly and economically attractive TWW treatment solutions is urgently needed. The aerobic granular sludge (AGS) technology, considered the next generation of wastewater treatment, represents a potential solution. This technology, implemented under the trade name Nereda®, consists in a sequencing fed-batch process with a simultaneous plug-flow feeding and effluent discharge step, an aeration stage and a settling stage (Pronk et al. 2015), allowing the simultaneous removal of chemical oxygen demand (COD), nitrogen and phosphate by AGS in a single sequencing batch reactor (SBR; de Kreuk et al. 2005). AGS consists of aerobic granules (AG), which are aggregates of microbial origin that can settle significantly faster than activated sludge flocs, allowing a good sludge-water separation, high biomass retention in the reactor, diverse microbial communities, high conversion capacities and high resistance towards toxic substances (Franca et al. 2018; Xia et al. 2018). Following the successful establishment of this innovative process as a sustainable and cost-effective treatment for municipal wastewater (Pronk et al. 2015), future directions include the application of the AGS technology to a wider range of wastewaters, namely those generated by the textile industry. In fact, recent reviews on the state of the art of AGS technology (Nancharaiah and Reddy 2018; Nancharaiah and Sarvajith 2019; Rollemberg et al. 2018) referred a few studies using AGS for the removal of azo dyes, highlighting textile wastewater treatment as a promising future AGS application. Aiming to explore the potential treatment of effluents from the textile industry using the AGS technology, an up-to-date review of the existing literature on AGS application to TWW treatment is herein presented, with a focus on the removal of two important TWW pollutants, azo dyes and silver nanoparticles (AgNP). The present review is the first to specifically focus on this potential field of AGS application, providing an updated and complete summary of the peer-reviewed studies conducted on textile dye and engineered nanoparticles (ENP) removal by AGS. The studies here gathered are specifically discussed in terms of AGS stability, biodecolorization mechanism and fate of azo dye breakdown products, providing a new perspective on the systems' treatment efficiency.

To contextualize, the main environmental problems raised by the azo dyes, including those associated with their toxic breakdown products (aromatic amines), are initially described. Among the possible solutions for azo dye removal from wastewater, studies focused on azo dye biodegradation (and sulfonated aromatic amine fate) in anaerobic–aerobic bioreactors are reviewed, namely highlighting those employing the novel AGS technology. In addition to the azo dyes, a separate section is dedicated to AgNP, which have been increasingly used by the textile industry and represent a novel concern regarding the environmental impact of the textile sector. Specifically, data regarding the presence of these ENP in TWW is presented and studies focused on AgNP fate and effects during wastewater treatment, namely in AGS SBR systems, are reviewed.

2 Azo dyes in textile wastewater (TWW)

2.1 Environmental impact and treatment solutions

Nearly two-thirds of the world annual dyestuff production are consumed by the textile industry, up to 50% of which has been estimated to reach the environment (Holkar et al. 2016; Rangabhashiyam et al. 2013; Rawat et al. 2016). Worldwide, 280,000 tons of textile dyes have been reported to be yearly discharged in textile industrial effluents, due to inefficient dye fixation processes onto the fibers (Raman and Kanmani 2016; Singh et al. 2015; Solís et al. 2012). Synthetic dyes are designed to have high durability, which gives them high stability in water and a recalcitrant nature, resistant to biodegradation. Therefore, conventional biological wastewater treatment processes fail in efficiently removing textile dyes from wastewaters, potentially leading to their long-term persistence in natural water bodies (Dasgupta et al. 2015; dos Santos et al. 2007).

Azo dyes account for more than 70% by weight of all dyestuffs used worldwide (Rawat et al. 2016) and represent the largest class of synthetic colorants applied in textile processing (approximately 80% by weight), consequently being the most commonly released into the environment (Saratale et al. 2011; Singh et al. 2015). Structurally, azo dyes are complex aromatic compounds characterized by the presence of one or more azo groups, linked to phenyl and naphthyl groups, which are usually substituted with some combinations of functional groups (Saratale et al. 2011). In addition to the previously described negative impact caused by the discharge of colored effluents into natural water bodies, azo dyes further threaten the flora, fauna and humans, owing to the toxicity, mutagenicity and carcinogenicity of some dyes and their breakdown products (Hisaindee et al. 2013; Solís et al. 2012). In fact, under certain environmental conditions, namely under low DO concentrations, the natural remediation potential of ecosystems may lead to partial degradation of these compounds through reductive cleavage of the azo bond, originating metabolites that can be more toxic than the original dye, specifically aromatic amines (Pinheiro et al. 2004; Rawat et al. 2016).

In terms of color removal from textile wastewater, decolorization occurs either by breaking down the dye molecule (at least partially) or by transferring it onto the sludge fractions. The latter can potentially contaminate the soil or the air, if disposed of into landfills or incinerated (Nimkar 2018). Previous review articles (Collivignarelli et al. 2019; Dasgupta et al. 2015; Fatima et al. 2017; Holkar et al. 2016; Raman and Kanmani 2016; Sen et al. 2016; Solís et al. 2012; Verma et al. 2012) have focused on different methods to treat colored TWW, namely oxidation methods (cavitation, Fenton processes, photocatalytic oxidation, chemical oxidation such as ozonation and peroxidation), physical methods (adsorption, coagulation/flocculation and membrane filtration) and biological methods (using fungi, algae, bacteria, and microbial fuel cells). In general, the implementation of the physico-chemical methods for color removal has inherent drawbacks, such as high cost due to intense energy demand or excessive chemicals use, transfer of contaminants without transformation, generation of high volumes of concentrated, polluting sludges requiring safe disposal, inefficient removal of recalcitrant azo dyes and their metabolites, as well as formation of hazardous by-products (Forgacs et al. 2004; Saratale et al. 2011). Regarding biological methods, biodecolorization can occur either via biosorption on microbial cells and/or via biodegradation (Solís et al. 2012). In fact, although azo dyes are generally considered as xenobiotic compounds and recalcitrant to aerobic biodegradation (namely during treatment with conventional activated sludge, CAS), several microorganisms are able to transform azo dyes into colorless breakdown products (partial biodegradation), or even to completely mineralize these metabolites (total biodegradation), under certain environmental conditions (Pearce et al. 2003; Stolz 2001; van der Zee and Villaverde 2005).

2.2 Anaerobic–aerobic biotreatment systems for azo dye biodegradation

2.2.1 Basic aspects

In contrast to conventional activated sludge aerobic wastewater treatment methods, anaerobic systems provide the optimal environment for azo dye decolorization through the reductive cleavage of the azo bond (dos Santos et al. 2007), but the resulting aromatic amines are resistant to further anaerobic mineralization (except for few, simple aromatic amines; Kalyuzhnyi et al. 2000; Pandey et al. 2007; Razo-

Flores et al. 1997). Conversely, owing to the potential further degradation of these azo dye breakdown products under aerobic conditions (Pinheiro et al. 2004), promising systems for the complete biodegradation of azo dyes are based on a combination of anaerobic and aerobic processes (van der Zee and Villaverde 2005). According to this approach, bacterial azo dye biodegradation generally proceeds in two stages: (1) the anaerobic phase, responsible for color removal through reductive cleavage of the azo bond, resulting in the formation of generally colorless, but potentially hazardous, aromatic amines; (2) the aerobic phase involving further degradation of aromatic amines (van der Zee and Villaverde 2005). Furthermore, the combination of anaerobic and aerobic conditions can allow the effective removal of nutrients (nitrogen and phosphorus). In addition to the removal of high organic loads during the anaerobic process, the residual biochemical oxygen demand (BOD) can be further eliminated under aerobic conditions (Delée et al. 1998).

Different anaerobic–aerobic reactor system approaches for treating azo dye-laden TWWs have been extensively reviewed (Sarayu and Sandhya 2012; van der Zee and Villaverde 2005). The anaerobic–aerobic treatments can occur sequentially (continuously in separate vessels, or in the same reactor by physical or temporal separation of anaerobic and aerobic phases), or simultaneously (based on the principle of limited oxygen diffusion in microbial biofilms, which contain anaerobic zones within aerobic bulk phases; Stolz 2001). Integrated anaerobic–aerobic bioreactors, where aerobic and anaerobic conditions are combined in a single reactor can generally enhance the overall degradation efficiency, are cost effective and have reduced footprints. In this context, sequential anaerobic–aerobic systems such as anaerobic–aerobic SBRs have been mostly employed in the study of TWW biological treatment, offering a compact layout, operational flexibility and simplicity (Lourenço et al. 2001).

Irrespective of the system configuration employed, high color removal yields (70–100%) were achieved under anaerobic conditions provided an electron donor (*e.g.*, biodegradable carbon source) was present and competing electron acceptors (*e.g.*, oxygen, nitrate, nitrite) were limited to low concentrations (van der Zee and Villaverde 2005). In contrast, successful reports on aerobic degradation of aromatic amines involved culture enrichment in specialized aerobes, with a very narrow substrate range (Pinheiro et al. 2004). In practice, several studies showed that activated sludge systems are not always able to aerobically degrade aromatic amines resulting from previous anaerobic azo dye reduction (van der Zee and Villaverde 2005). In fact, the biodegradation potential of aromatic amines can range from highly degradable to non-biodegradable, depending on the position, type and number of substituents in the aromatic ring (Lourenço et al. 2003). Moreover, the difficulty in achieving complete azo dye biodegradation is commonly associated with the generation of recalcitrant sulfonated aromatic amines, owing to the hydrophilic nature of the sulfonate group (Lourenço et al. 2009; Tan et al. 2005). Few pure cultures and microbial consortia capable of degrading specific sulfonated naphthylamines have been isolated (Barsing et al. 2011; Hong et al. 2007; Juárez-Ramírez et al. 2012; Pandey et al. 2007). In fact, biodegradation of this type of compounds has mostly been demonstrated for relatively simple sulfonated aminobenzene and aminonaphthalene compounds (Haug et al. 1991; Tan et al. 2000), often requiring extensive biomass acclimation (Tan et al. 2005). Accordingly, unadapted microbial populations in activated sludge were shown to fail in completely degrading sulfonated naphthalenes (Nortemann et al. 1986). This difficulty in mineralizing azo dye reduction products under aerobic conditions has generally been attributed to the lack of an adequate aerobic microbial population capable of metabolizing such compounds (Tan et al. 1999a). Therefore, the cultivation of microbial consortia capable of efficiently degrading a mixture of aromatic amines has been suggested for bioaugmentation of aerobic treatment units (Pandey et al. 2007). These specialized microbial communities can be selected if persistently exposed to the aromatic substrates to induce metabolic adaptation (Tan et al. 2005).

Aerobic metabolization of aromatic amines is generally suggested to occur via a hydroxylation pathway involving a ring-opening mechanism in the presence of oxygen, catalyzed by oxygenases (Pereira et al. 2015; Stolz and Knackmuss 1993). However, upon exposure to aerobic conditions, a large fraction of azo dye metabolites (especially aromatic amines *ortho*-substituted with hydroxyl groups), are susceptible to autoxidation, as oxygen reacts with the aromatic products via free radical mechanisms,

oxidizing hydroxyl and amino groups to quinines and quinine imines (Barsing et al. 2011; Kudlich et al. 1999). These compounds can undergo dimerization or polymerization, generally yielding thermodynamically stable, soluble, colored oligomers (or, less commonly, insoluble polymers) resistant to further biodegradation and potentially toxic and mutagenic (Field et al. 1995; Kudlich et al. 1999; Solís et al. 2012). These chemical, spontaneous reactions make it difficult to predict the fate of aromatic amines during anaerobic–aerobic treatment of azo dyes (van der Zee and Villaverde 2005). Moreover, the competition between biodegradation and autoxidation (especially regarding *o*-aminohydroxynaphthalenes) should be further assessed, as well as the possibilities for biological mineralization of autoxidation products (Stolz 2001). Given this scenario, complete biomineralization of azo dyes is still the focus of much research in the context of the environmental impact of textile industry wastewater.

According to a recent review (Raman and Kanmani 2016), most studies indicate complete removal of azo dyes from TWW to be achieved simply based on successful decolorization results, which is not an accurate conclusion. In contrast with the notable success in the anaerobic decolorization stage, information regarding the fate of the breakdown aromatic amines during the aerobic stage, when available, revealed that most of these amines were not aerobically degraded, being considered a health hazard (Pinheiro et al. 2004; van der Zee and Villaverde 2005). In fact, the few studies monitoring the removal of total organic carbon, as well as dye intermediates or end products formed, generally conclude that only partial mineralization of the textile dye is achieved (Raman and Kanmani 2016). As previously mentioned, incomplete azo dye mineralization is commonly associated with the production of sulfonated aromatic amines, which are among the most common products of bacterial decolorization of azo dyes (Pandey et al. 2007). Moreover, when their removal was reported, the process (adsorption, biological or chemical transformations) was not clear, the aerobic fate of (sulfonated) aromatic amines thus deserving more investigation (van der Zee and Villaverde 2005).

2.2.2 *Fate of sulfonated aromatic amines in anaerobic–aerobic bioreactors*

This section presents an overview of studies in which azo dye-laden TWW treatment was carried out by mixed bacterial cultures in bioreactor systems, including an anaerobic treatment stage for the reductive cleavage of azo dyes, followed by an aerobic stage for degradation of potentially toxic, colorless breakdown aromatic amines. This review specifically focuses on studies addressing the formation and fate of sulfonated aromatic amines. Accordingly, Table 1 specifies the operational conditions used in the different bioreactor systems, as well as the main treatment performance indicators in terms of COD, color and aromatic amines removal, while Table 2 further specifies the conclusions derived by the authors regarding the fate of aromatic amines. Among the reviewed studies on the biodegradation of sulfonated azo dyes in anaerobic–aerobic bacterial systems (Table 1), different aromatic amine fates were reported: mineralization (Balapure et al. 2015; Işik and Sponza 2004a; Libra et al. 2004; Sponza and Isik 2002), nearly complete biodegradation (FitzGerald and Bishop 1995; Forss and Welander 2011; Sponza and Işik 2005b), further/partial degradation (Jonstrup et al. 2011; Paździor et al. 2009) or, more specifically, degradation to non-aromatic, polar compounds (Khehra et al. 2006; O'Neill et al. 2000), incomplete (Shaw et al. 2002) or no mineralization (Libra et al. 2004; Lourenço et al. 2003; Lourenço et al. 2009).

The reported cases of partial or complete aerobic removal of the azo dye-derived aromatic amines (Table 2) were mostly based on indirect observations, such as: decreases in ultraviolet (UV) absorbance (Dafale et al. 2008; Jonstrup et al. 2011; Shaw et al. 2002; You and Teng 2009), toxicity (Balapure et al. 2015; Işik and Sponza 2004b) and total aromatic amines levels measured by diazotization-based colorimetric methods (the standard usually corresponding to one of the expected metabolites; Spagni et al. 2010; Sponza and Işik 2005b); the decrease in overall high-performance liquid chromatography (HPLC) peak areas (including unidentified peaks) and shift of peaks to lower retention times during the aerobic phase, indicating the formation of less aromatic and more polar compounds (Koupaie et al. 2011); the disappearance of signals at low field zone in ^{1}H NMR (proton nuclear magnetic resonance) analysis

Table 1 Sequential anaerobic–aerobic reactor systems treating azo dye-laden textile wastewater

Bioreactor system[a]	Seed sludge[b]	HRT (h)[c]			SRT (d)[d]	Textile wastewater			Removal performance (%)			Method for AA analysis[i]	References
		An	Ae	Total		Type[e]	Substrate[f] (COD, mg O_2 L^{-1})	Azo dyes[g] (mg L^{-1})	COD	Color	AA[h]		
Anaerobic fixed film fluidized bed reactor + **Aerobic** reactor	An-1 Ae-1	31	3.1	43	n.i.	S	Trout chow, BE, YE, peptone (170)	AO10, AR14 or AR18 (10)	85	65–90	> 99 (An)	LC–MS	FitzGerald and Bishop (1995)
Anaerobic SBR + **Aerobic** MB-SBBR	An-2 Ae-1	66 *21	66 *22.5	132 *48	n.i.	S	Glucose, lactose (2950–3725)	AR18 (100–1000)	80	98	> 84 (4A1NS) 50–60 (Total)	HPLC	Koupaie et al. (2011)
Integrated **anaerobic–aerobic** fixed bed SBBR	An + Ae	*14	*8	168 *24	n.i.	S	Glucose, lactose (1030–1045)	AR18 (100)	> 92	> 95	> 96 (4A1NS) > 51 (Total)	HPLC	Koupaie et al. (2013)
(Anoxic) fixed film column reactor + **Aerobic** CSTR	BC	12	n.i.	n.i.	n.i.	S	Glucose (1630)	AR88 (100)	95	98	n.q.	UV–vis, TLC ^{1}H NMR	Khehra et al. (2006)
Anaerobic UASB reactor + **Aerobic** CSTR	An-3 Ae-2	15	55	70	18 (Ae)	S	Glucose (2000)	DBk38 (3200)	84	86	52 (TAA)	DCM1 GC–MS	Sponza and Işik (2005a)
Anaerobic UASB reactor + **Aerobic** CSTR	An-3 Ae-3	86	432	518	86 (An)	S	Glucose (4100)	DBk38 (3200)	92	94	86 (TAA) 45 (Benzidine)	HPLC–DAD GC–MS, DCM1	Işik and Sponza (2004b)
Anaerobic UASB reactor + **Aerobic** CSTR	An-3 Ae-2	19	67	86	12–16 (Ae)	S	Glucose (3000)	DR28 (4000)	88	99	91 (TAA)	DCM1	Işik and Sponza (2003)
Anaerobic UASB reactor + **Aerobic** CSTR	An-3 Ae-3	1728	432	2160	n.i.	S	Glucose (5377)	DR28 (3200)	91	96	97 (TAA) 91 (Benzidine)	HPLC–DAD GC–MS,DCM1	Sponza and Işik (2005b)
3 biofilter reactors: 2 **Anaerobic** + 1 **Aerobic**	FR	232	116	348	n.i.	S	n.i.	Mixture A (400; 200 each)	n.i.	86–90	n.q.	LC–MS	Forss and Welander (2011)
Anaerobic UASB reactor + **Aerobic** CSTR	An-3 Ae-2	100	360	460	25 (Ae)	S	Starch, CMC, acetate, glucose (4214 ± 241)	Mixture B (250; 50 each)	97	91	70–85 (TAA)	DCM1	Işik and Sponza (2008)
Anaerobic UASB reactor + **Aerobic** CSTR	An-3 Ae-2	30	108	138	n.i.	R	Cotton textile mill WW + glucose (600–2000)	Mixture B (100–500)	40–85	39–81	37–87 (TAA)	HPLC DCM1	Işik and Sponza (2004a)

Table 1 continued

Bioreactor system[a]	Seed sludge[b]	HRT (h)[c]			SRT (d)[d]	Textile wastewater			Removal performance (%)			Method for AA analysis[i]	References
		An	Ae	Total		Type[e]	Substrate[f] (COD, mg O_2 L^{-1})	Azo dyes[g] (mg L^{-1})	COD	Color	AA[h]		
Microaerophilic fixed film reactor (DO ~ 0.07 mg L^{-1})	BC acclim. to RB160	n.i.	n.i.	24	n.i.	S	Starch, glucose (7200)	Mixture C (300; 50 each)	98	100	n.q.	FTIR ^{1}H NMR GC–MS	Balapure et al. 2015
Anoxic reactor + **Aerobic** reactor	BC acclim. to RBk5	n.i.	n.i.	24	n.i.	S	Glucose (2000)	RBk5 (100)	> 90	> 90	73 (Total)	UV–vis	Dafale et al. (2008)
Anaerobic UASB reactor + **Aerobic** CSTR	An-3 Ae-2	*30	108	138	11 (Ae)	S	Glucose (3000)	RBk5 (100)	96	95	n.q.	UV–vis	Sponza and Isik (2002)
Anaerobic SBR + **Aerobic** MBR	TS	48 *21.5	24	72	n.i.	S	Milk powder, sucrose, acetate (300)	RBk5 (6)	98	83	62 (Total)	UV–vis	You and Teng 2009
Anaerobic RDR + **Aerobic** RDR	n.i.	15*	7.5*	n.i.	n.i.	S	YE, acetate (580 mg L^{-1} as DOC)	RBk5 (530)	80–90	65	n.q.	LC–MS	Libra et al. (2004)
Anaerobic biofilter + **Anoxic** reactor + **Aerobic** MBR	An-1 Ae-1	n.i.	n.i.	24–94	80–100	S	Glucose (800)	RO16 (5–38)	79	90	n.q.	DCM2	Spagni et al. (2010)
Anaerobic–Aerobic SBR or **Anaerobic** + **Aerobic** SBRs	MS	48 *19.3	96 *3	144 *24	n.i.	R+ S	Cotton dyeing WW, acetate, peptone (570)	RR120 (n.i.)	93–98 95–98	93–98 92–97	n.q.	HPLC	Paździor et al. (2009)
Anaerobic UASB reactor + **Aerobic** reactor	An-4 Ae-4	24	19	n.i.	n.i.	S	Modified starch, acetate (3343)	RR141 (450)	85	75	n.q.	HPLC	O'Neill et al. (2000)
Anaerobic–aerobic SBR	An-5	*18.5	*0.5	62 *24	n.i.	S	Polyvinyl alcohols (3916)	RR5 (533)	66	94	n.q.	UV–vis	Shaw et al. (2002)
Anaerobic–aerobic SBR	Ae-4	*9–13	*8–12	26–53 *24	n.i.	S	Modified starch (750–1500)	RV5 (C_i, 90)	80	90	n.q.	HPLC	Lourenço et al. (2003)
Anaerobic–aerobic SBR + **Aerobic** SBR	Ae-4	*9	*12	52.8 *24	15	S	Modified starch (1000)	RV5 (C_i, 100)	38	90	n.q.	HPLC	Lourenço et al. (2009)
Anaerobic–aerobic SBR	Ae-5	*12	*12	*24	10	S	Glucose (1000)	RV5 (100)	> 75	89	92 (BBA) 64 (NBA)	HPLC[&]	Çinar et al. (2008)

Table 1 continued

Bioreactor system[a]	Seed sludge[b]	HRT (h)[c]			SRT (d)[d]	Textile wastewater			Removal performance (%)			Method for AA analysis[i]	References
		An	Ae	Total		Type[e]	Substrate[f] (COD, mg O_2 L^{-1})	Azo dyes[g] (mg L^{-1})	COD	Color	AA[h]		
Anaerobic biofilm reactor + **Aerobic** reactor	An-1 Ae-1 or Ae-6	24–72	n.i.	n.i.	n.i.	S	Glucose (1000)	Remazol Red RR (100)[#]	82–95	98	30 (Total)	UV–vis HPLC	Jonstrup et al. (2011)

[a]CSTR: continuous stirred-tank reactor, DO: dissolved oxygen, MB: moving bed, MBR: membrane bioreactor, RDR: rotating disc reactor, SBBR: sequencing batch biofilm reactor, SBR: sequencing batch reactor, UASB: upflow anaerobic sludge blanket

[b]Acclim.: acclimatized; Ae: seed sludge in the aerobic reactor; Ae-1: activated sludge from a municipal wastewater treatment plant (WWTP); Ae-2: activated sludge from a dye industry; Ae-3: activated sludge from a lab scale CSTR treating molasses; Ae-4: activated sludge from a WWTP treating mixed municipal/industrial wastewater; Ae-5: Activated sludge from a textile WWTP; Ae-6: Aerobic reactor: activated sludge from a nitroaromatics industry or a textile industry; Ae: seed sludge in the anaerobic reactor; An-1: sludge from an anaerobic digester treating municipal WWTP; An-2: granulated anaerobic sludge from a UASB reactor treating dairy factory; An-3: partially granulated sludge from a methanogenic reactor of an yeast baker factory; An-4: granules from a paper-pulp processing plant; An-5: Anaerobic granules from a UASB reactor treating wastewater from a potato processing factory; An + Ae: mixture of anaerobic granular sludge from a full-scale UASB reactor and activated sludge from a municipal WWTP; BC: bacterial consortium isolated from waste disposal sites of textile processing industries; FR: forest residues (soft wood shavings); MS: surplus activated sludge and fermented sludge from a methane fermentation stage of a municipal WWTP; n.i.: not indicated; RB160: reactive blue 160; RBk5: reactive black 5; TS: sludge from industrial WWTP treating highly colored textile wastewater

[c]Ae: aerobic stage; An: anaerobic stage; n.i.: not indicated; HRT: Hydraulic retention time; *duration, in hours, of the anaerobic reaction phase, aerobic reaction phase or total cycle indicated in the respective An, Ae and Total columns (only indicated for SBRs and SBBRs)

[d]Ae: aerobic stage; An: anaerobic stage; n.i.: not indicated: duration; SRT: sludge retention time

[e]S: simulated textile wastewater; R: real textile wastewater

[f]BE: beef extract; CMC: carboxymethyl cellulose; DOC: dissolved organic carbon; n.i.: not indicated; WW: wastewater; YE: yeast extract

[g]AO: acid orange; AR: acid red; C_i: initial dye concentration in the reactor; DBk: direct black; DBr: direct brown; DR: direct red; DY: direct yellow; RBk: reactive black; RO: reactive orange; RR: reactive red; RV: reactive violet; [#]Other reactive azo dyes (remazol blue RR and remazol yellow RR) were used in batch tests; Mixture A: mixture of RBk5 and RR2; Mixture B: mixture of RBk5, DR28, DBk38, DBr2 and DY12; Mixture C: mix of RR2, RR198, RR120, RB160, RB13 and RB172

[h]4A1NS: 4-amino-naphthalene-1-sulfonic acid; AA: aromatic amines; An: Anaerobic stage; BBA: benzene-based amine; NBA: naphthalene-based amine; n.q.: not quantified; TAA: total aromatic amines; Total: total azo dye metabolites

[i]DAD: diode-array detection; DCM1: diazotization-based colorimetric method 1 [colorimetric analysis of total aromatic amines after reaction with 4-dimethylamino benzaldehyde-HCl; quantification of total aromatic amines (TAA) using benzidine as standard]; DCM2: diazotization-based colorimetric method 2 [diazotization-coupling reaction with or N-(1-naphthyl)ethylenediamine; quantification of TAA using sulfanilic acid (chemical structure similar to one of the expected AA) as standard]; FTIR: Fourier-transform infrared spectroscopy; GC: gas chromatography; ^{1}H NMR: proton nuclear magnetic resonance; HPLC: high-performance liquid chromatography; LC: liquid chromatography; MS: mass spectrometry; TLC: thin layer chromatography; UV–vis: ultraviolet–visible spectrophotometry; [&]Relative quantification by attributing the maximum aromatic amine concentration (100%) to the highest peak

Table 2 Comments on the fate of aromatic amines (AA) in sequential anaerobic–aerobic reactor systems treating azo dye-laden textile wastewater (operational details in Table 1)

Azo dyes[a]	AA removal (%)[b]	Method[c]	Authors comments regarding AA fate[d]	Reference
AO10 AR14 AR18	> 99 (An)	LC–MS	AA quantitative analysis using standards for the respective metabolites or compounds having the same chemical formula but similar structure Low metabolites recovery (< 1%) at the end of An. Adsorption to biomass and low recovery efficiencies have been ruled out Further studies must be conducted to confirm the hypothesized (> 99%) anaerobic biodegradation of the intermediates	FitzGerald and Bishop (1995)
AR18	> 84 (4A1NS) > 50 (Total)	HPLC	Except for 4A1NS, the other intermediates were not quantified due to unavailability of authentic standards Overall HPLC peak area analysis revealed that > 50% of total dye metabolites detected at the end of the An were removed during the Ae The HPLC peak area decreased and shifted to lower RT during the Ae, indicating the formation of less aromatic and more polar compounds	Koupaie et al. (2011, 2013)
AR88	n.q.	UV–vis, TLC ^{1}H NMR	.^{1}H NMR analysis indicated complete loss of aromaticity from the azo dye after sequential anoxic-aerobic treatment TLC and^{1}H NMR revealed that the aromatic intermediates produced under anoxic conditions were degraded to non-aromatic metabolites in the Ae	Khehra et al. (2006)
DBk38	52 (TAA)	DCM1 GC–MS	Two of the four azo dye breakdown products (benzidine, aniline) were recovered (95%) in the An, but not all were further mineralized in the Ae Low levels of AA and absence of breakdown products in GC–MS spectra indicated that most of the AA were metabolized Comparison between UV–vis scans of benzidine with the reactors' influent and effluent indicated the complete mineralization of TAA	Sponza and Işik (2005a)
	86 (TAA) 45 (Benzidine)	HPLC–DAD GC–MS DCM1	Only two of the four expected dye metabolites were detected (namely benzidine), the authors suggesting that part of AA were removed in the An The area of the two HPLC peaks significantly decreased during the Ae, but GC–MS showed that the azo dye was not completely mineralized Toxicity of the Ae effluent were significantly lower than the An effluent, suggesting complete aerobic mineralization of carcinogenic amines The authors concluded that dyes could be mineralized in the system, despite some residual presence of benzidine in the final effluent	Işik and Sponza (2004b)
DR28	97 (TAA) 91 (Benzidine)	HPLC–DAD GC–MS DCM1	Only 25% (as TAA) of the expected dye metabolites were recovered at the end of the An, the authors suggesting that 75% were removed in the An The TAA recovered at the end of the An could be removed in the Ae (91%). Only benzidine was identified by HPLC and GC–MS analysis The decrease in the area of two HPLC peaks indicated partial aerobic degradation of benzidine (confirmed by GC–MS) and an unknown metabolite The authors concluded that the system allowed nearly complete biodegradation of the benzidine-based azo dye, leading to detoxification	Sponza and Işik (2005b)
Mixture A	n.q.	LC–MS	Two metabolites were degraded to below the DL in the Ae, with no trace of AA polymerization or dimerization, their mineralization being suggested The structure of the two detected metabolites could not be identified, owing to the lack of standardized MS-libraries for LC	Forss and Welander (2011)

Table 2 continued

Azo dyes[a]	AA removal (%)[b]	Method[c]	Authors comments regarding AA fate[d]	Reference
Mixture B	37–87 (TAA)	DCM HPLC	The authors concluded that the azo dyes were reductively decolorized in the An and mineralized in the Ae	Işik and Sponza (2004a)
			Benzidine, produced from the azo bond cleavage in the An, was effectively removed in the Ae, as confirmed by HPLC with authentic standard	
Mixture C	n.q.	FTIR ^{1}H NMR GC–MS	Loss of aromaticity or fission of benzene rings from the dyes during the Ae was indicated by FTIR and by the absence of peaks in the UV region	Balapure et al. (2015)
			GC–MS showed that lower molecular weight aliphatic compounds were formed, which indicated complete cleavage of AA into aliphatic compounds	
			The disappearance of all signals at low field zone in ^{1}H NMR analysis indicated the complete mineralization of dyes	
			Higher MW compounds were not detected, indicating the complete mineralization of the WW, further supported by the decrease in toxicity	
RBk5	73 (Total)	UV–vis	The UV–vis spectral changes represent the disappearance of the azo dye and concomitant formation of metabolites during the anoxic reaction	Dafale et al. (2008)
			The decrease in the UV major absorbance peak indicated that the AA formed in the anoxic reactor were significantly removed (73%) in the Ae	
	n.q.	UV–vis	The slight increase in the color during the Ae suggested the occurrence of oxidation or polymerization of intermediate compounds formed in the An	Sponza and Isik (2002)
			The authors concluded that the released intermediates were mineralized in the Ae	
	62 (Total)	UV–vis	UV–vis results showed that the AA intermediate metabolites formed in the An were further mineralized in the Ae (62% of degradation)	You and Teng (2009)
	n.q.	LC–MS	Partial mineralization of the fully hydrolyzed azo dye was achieved	Libra et al. (2004)
			Specifically, one of AA was mineralized (p-ABHES), but the other metabolite (TAHNDS) was not removed in the aerobic stage	
RO16	n.q.	DCM2	At least the sulfonated AA formed under anaerobic conditions were recalcitrant to biodegradation	Spagni et al. (2010)
RR120	n.q.	HPLC	Two HPLC peaks were formed in the An, one of which corresponded to orthanilic acid	Paździor et al. (2009)
			Orthanilic acid (confirmed by standard) was further biodegraded under aerobic conditions, while the second peak was recalcitrant to biodegradation	
			The orthanilic acid was further degraded in the Ae of the two-stage anaerobic/aerobic system, but not in the integrated anaerobic–aerobic SBR	
RR141	n.q.	HPLC	The HPLC-detected compounds (none corresponding to the expected AA) were aerobically removed or converted to highly polar compounds.	O'Neill et al. (2000)
			Toxicity of the effluent was eliminated after the Ae	
			This study qualitatively showed that AA-derivatives formed during the An were degraded into more polar, non-aromatic by-products during the Ae	
RR5	n.q.	UV–vis	The intensity of peaks in the UV region was slightly reduced during the Ae, the authors concluding that AA were not completely mineralized	Shaw et al. (2002)

Table 2 continued

Azo dyes[a]	AA removal (%)[b]	Method[c]	Authors comments regarding AA fate[d]	Reference
RV5	n.q.	HPLC	The two AA resulting from the anaerobic azo bond reduction were detected by HPLC analysis, but not mineralized during the subsequent Ae	Lourenço et al. 2003, 2009
			Despite interconversions between the BBA and an unknown metabolite, no effective biodegradation was observed along the operation (> 810 days)	
			Prolonging the Ae resulted in partial conversion of the BBA into the unknown metabolite, but the NBA remained practically unchanged	
Remazol Red RR[#]	30 (Total)	UV–vis HPLC	Partial degradation of AA during the Ae was suggested by the 30% reduction in the UV peak absorbance level	Jonstrup et al. (2011)
			Four HPLC peaks (not identified) were detected at the end of the An, three of which were absent at the end of the Ae	
			Batch tests using sludge acclimatised to nitroaromatics or azo dyes revealed that only partial degradation of AA from Remazol Red RR and from Remazol Blue RR was achieved, while autoxidation of Remazol Yellow RR metabolites occurred during the Ae, forming a recalcitrant product	

[a]AO: acid orange; AR: acid red; DBk: direct black; DR: direct red; RBk: reactive black; RO: reactive orange; RR: reactive red; RV: reactive violet; [#]other reactive azo dyes (remazol blue RR and remazol yellow RR) were used in batch tests; Mixture A: mixture of RBk5 and RR2; mixture B: mixture of RBk5, DR28, DBk38, DBr2 and DY12; mixture C: Mix of RR2, RR198, RR120, RB160, RB13 and RB172

[b]4A1NS: 4-amino-naphthalene-1-sulfonic acid; AA: aromatic amines; An: anaerobic stage; Total: total azo dye metabolites; n.q.: not quantified; TAA: total aromatic amines

[c]DAD: diode-array detection; DCM1: Diazotization-Based Colorimetric Method 1 (colorimetric analysis of total aromatic amines after reaction with 4-dimethylamino benzaldehyde-HCl; quantification of total aromatic amines (TAA) using benzidine as standard); DCM2: diazotization-based colorimetric method 2 (diazotization-coupling reaction with or N-(1-naphthyl)ethylenediamine; quantification of TAA using sulfanilic acid (chemical structure similar to one of the expected AA) as standard); FTIR: Fourier-transform infrared spectroscopy; GC: gas chromatography; ^{1}H NMR: proton nuclear magnetic resonance; HPLC: high-performance liquid chromatography; LC: liquid chromatography; MS: mass spectrometry; TLC: thin layer chromatography; UV–vis: ultraviolet–visible spectrophotometry; [&]relative quantification by attributing the maximum aromatic amine concentration (100%) to the highest peak

[d]4A1NS: 4-amino-naphthalene-1-sulfonic acid; AA: aromatic amines; Ae: aerobic stage; An: anaerobic stage; BBA: benzene-based amine; DL: detection limit; FTIR: fourier-transform infrared spectroscopy; GC: gas chromatography; ^{1}H NMR: proton nuclear magnetic resonance; HPLC: high-performance liquid chromatography; LC: liquid chromatography; MS: mass spectrometry; MW: molecular weight; NBA: naphthalene-based amine; p-ABHES: p-aminobenzene-2-hydroxyethylsulfonic acid; RT: retention times; TAA: total aromatic amines; TAHNDS: 1,2-ketimino-7-amino-8-hydroxynaphthalene-3,6-disulfonic acid; TLC: thin layer chromatography; UV–vis: ultraviolet–visible spectrophotometry; WW: wastewater

indicating the loss of aromaticity (Balapure et al. 2015; Khehra et al. 2006); the decrease in FTIR (Fourier-transform infrared spectroscopy) peaks associated with aromatic structures (Balapure et al. 2015); the detection of lower molecular weight aliphatic compounds in gas chromatography coupled with mass spectrometry (GC–MS; Balapure et al. 2015). Moreover, quantification of the expected azo dye intermediates through chromatographic techniques is limited to the availability of the respective standard. Among the reviewed studies (Table 1), authentic standards have been used for 4-amino-naphthalene-1-sulfonic acid (4A1NS; Koupaie et al. 2011, 2013), benzidine (Işik and Sponza 2004a, b; Sponza and Işik 2005b), orthanilic acid (Paździor et al. 2009), *p*-aminobenzene-2-hydroxyethylsulfonic acid and 1,2-ketimino-7-amino-8-hydroxynaphthalene-3,6-disulfonic acid (Libra et al. 2004). Except for the latter, all of these metabolites were suggested to be mineralized in the aerobic phase, based on HPLC, liquid chromatography coupled with mass spectrometry (LC–MS) and GC–MS analyses. On the other hand, some aromatic

amines cannot be quantified due to the unavailability of an authentic standard. Moreover, the fate of unidentified metabolites generated along the treatment can be qualitatively assessed based on their chromatographic peak area variation (O'Neill et al. 2000; Sponza and Işik 2005b).

A sound comparison between studies testing the biodegradation of the same azo dye is difficult because of the differences in operational conditions. Although using different reactor system configurations, inocula and substrates, three studies focused on Reactive Black 5 (Table 2) reported that the aromatic amines resulting from the reductive cleavage of the azo dye were mineralized (Sponza and Isik 2002) or significantly removed during the aerobic stage, with an overall 62–73% removal yield (Dafale et al. 2008; You and Teng 2009). However, while these conclusions were based on UV–visible spectral results, another study using a more accurate method for analyzing the individual fate of azo dye metabolites (LC–MS; Libra et al. 2004), concluded that only one of the aromatic amines was mineralized, the other being recalcitrant under aerobic conditions. Regarding the treatment of Reactive Violet 5 (Table 1), biodegradation of the resulting aromatic amines was reported by Çinar et al. (2008), the aerobic removal yields being 92% for the benzene-based amine and 64% for the naphthalene-base amine, according to HPLC analysis. On the other hand, other studies specifically focused on the fate of these aromatic amines showed that despite the also observed decrease in the respective HPLC peak area, effective biodegradation of the benzene-based amine did not occur, as it was partially converted into an unknown metabolite (Lourenço et al. 2003, 2009). Moreover, the naphthalene-base amine remained practically unchanged in the latter studies, being considered recalcitrant under the employed conditions.

Contradictory conclusions regarding the biodegradation potential of the same azo dye in anaerobic–aerobic treatment systems may not only be attributable to differences in the operational conditions, but also to incomplete metabolite analysis or inaccurate data interpretation. For instance, owing to the low recovery of expected azo dye metabolites at the end of the anaerobic treatment, as detected by LC–MS or GC–MS, authors concluded that biodegradation of the intermediates occurred under anaerobic conditions (FitzGerald and Bishop 1995; Işik and Sponza 2004b; Sponza and Işik 2005b), which is unlikely. On the other hand, You and Teng (2009) stated that the azo dye metabolites formed in the anaerobic phase were further mineralized in the aerobic phase, based on a 62%-reduction in UV absorbance. Also based on UV–visible spectral analysis, Sponza and Isik (2002) finally concluded that the azo dye intermediates were aerobically mineralized, despite previously hypothesizing the occurrence of aromatic amine autoxidation and polymerization due to the slight increase in the color levels. Conversely, other studies using LC–MS or GC–MS reported mineralization of aromatic amines as the formation of higher molecular weight compounds was not observed, with no trace of aromatic amines polymerization or dimerization (Balapure et al. 2015; Forss and Welander 2011).

Overall, some studies suggested partial or even complete mineralization of the aromatic amines, while others reported that mineralization was not achieved because the formation of new intermediates was observed (Table 2). Moreover, the new metabolites, such as polymerization or dimerization products resulting from autoxidation of aromatic amines, may arise during the aerobic stage without being properly detected by HPLC, depending on the conditions of analysis. Overall, despite most of the reviewed studies further supporting the potential for biodegradation of sulfonated aromatic amines, clear evidence for complete azo dye mineralization was rarely provided, requiring further investigation and more conclusive data.

2.2.3 *Treatment of azo dye-laden TWW in AGS sequencing batch reactor (SBR) systems*

2.2.3.1 AGS potential for TWW Aiming to achieve complete mineralization of an azo dye, Kudlich et al. (1996) immobilized, in alginate beads, azo dye-reducing bacteria together with bacteria able to mineralize the reduction products. Following this unsuccessful attempt, the authors highlighted the need for a more rigid and mechanically stable material that would still allow the establishment of an oxygen gradient, similarly to biofilms. In this sense, Tan et al. (1999a) subsequently tested the use of anaerobic granular sludge as a self-immobilization system providing both anaerobic and aerobic microniches when operated under aerobic conditions. Yet, the aromatic amines formed upon azo dye reduction were

not further transformed in the presence of oxygen. This was attributed to the absence of a suitable aerobic microbial population within the anaerobic granular sludge capable of metabolizing aromatic amines. Therefore, the authors indicated that addition of adapted aerobic biomass would be probably required to achieve azo dye mineralization (Tan et al. 1999b). In this context, the solution for this problem might lie on AG, which are self-immobilized, dense aggregates mainly composed of bacteria and extracellular polymeric substances (EPS), and are considered as a special case of biofilm growth without carrier material (Beun et al. 1999). AG are commonly cultured in aerobic SBRs and their granular structure creates DO and substrate concentration gradients along the radial direction, leading to stratification in layers of different microenvironments (aerobic, anoxic, anaerobic) within each AG, thus allowing the co-presence of different types of microorganisms and metabolisms in the same tank (de Kreuk et al. 2005). As hypothesized by Manavi et al. (2017), the channels present within AG could be used for transport of dyes and organic substrates into the anaerobic core region of the granules, where (facultative) anaerobic bacteria would reduce azo dyes using the reducing equivalents resulting from the oxidation of the organic compounds. Subsequently, the AG channels would allow the resulting aromatic amines to migrate from the core to the aerobic outer layers of the AG, where they could be mineralized by aerobic bacterial populations (Manavi et al. 2017).

Overall, in addition to the general advantages over the conventional flocculent sludge, AGS has characteristics that might potentially promote the complete biomineralization of azo dyes. Specifically, the coexistence of aerobic and anoxic-anaerobic zones within the granules (Winkler et al. 2013) and their enhanced resistance to high organic loads and toxic recalcitrant compounds (Franca et al. 2018) might be advantageous for treating TWW. Furthermore, their superior capacity to biodegrade toxic and recalcitrant pollutants derives from the wide range of possible operational sludge retention time (SRT) values in AGS systems (de Kreuk and van Loosdrecht 2004). In fact, the operational SRT flexibility of AGS systems enables the presence of a more diverse microbial community within the SBR, namely slow-growing populations, whose activity may be advantageous for the degradation of recalcitrant compounds (Clara et al. 2005; Langford et al. 2005; Lourenço et al. 2015). In addition, results from previous studies using flocculent activated sludge for TWW treatment (Lourenço et al. 2000) suggest that systems with higher biomass retention capacity are probably advantageous for allowing the development of a more diverse microbial population capable of degrading a broader range of dyes. Accordingly, a study reported the biodegradation of a sulfonated aromatic amine (4A1NS), described as highly recalcitrant, through the use of biofilm reactors, which allow high biomass retention (Koupaie et al. 2013).

Although using the AGS technology for the treatment of high strength, dye-laden TWW offers great promise for the above mentioned reasons, only few reports have been published on the use of AGS SBRs for this specific application, most of which using synthetic TWW (Kodam and Kolekar 2014; Nancharaiah and Reddy 2018). Furthermore, although biodegradation and biosorption are generally reported as the dye removal processes in biological systems, the mechanisms and metabolic pathways occurring in AGS systems are still poorly addressed in the literature and deserve more investigation (Rollemberg et al. 2018).

2.2.3.2 TWW containing a mixture of dyes **Intermittent anaerobic–aerobic SBR** The first published study on this subject (Muda et al. 2010; Table 3) reported on the development of stable, mature AG with excellent settleability, in the presence of a mixture of dyes. In terms of treatment performance, the relatively low and inconsistent decolorization yields were attributed to insufficient microbial adaptation time to the recalcitrant dyes (20 days), to possible aerobic formation of colored autoxidation products from unstable aromatic amines and/or to color removal through adsorption of dyes to the biomass. In fact, as the formation of aromatic amines was not assessed, the decolorization process was uncertain, especially regarding the partial color removal observed under aerobic conditions (ca. 17%), which was suggested by the authors to derive from azo bond reduction within the anaerobic core of the AG. Moreover, despite not providing clear evidence, the authors attributed the high oxygen uptake rate (OUR) registered during the last aerobic stage to the mineralization of the (unassessed) aromatic amines.

Table 3 Summary of operational conditions and main results of studies employing aerobic granular sludge in the treatment of dye-laden textile wastewater

System[a]	H/D; V (L)[b]	VER (%)[c]	OLR[d]	HRT (h)[e]	SRT (d)[f]	Seed[g]	WW type (COD)[h]	Substrate[i]	Dye (mg L^{-1})[j]	Cycle[k]	
Int.An-Ae SBR	12.5; 4.0	50	2.4	n.i.	1.4–8.3	i	Dye-SWW (1270)	Glucose, ethanol, acetate	Mixture of dyes (50)	Total (6 h): F (5′) + An1* (0.7 h) + Ae1 (2.2 h) + An2* (0.7 h) + Ae2 (2.2 h) + S (5′) + D (5′)	
An-Ae SBR	20.0; 1.5	50	2.5	8	n.i.	i	Dye-SWW (1240)			Total (8 h): F (5‘) + An# (3.8 h) + Ae (3.8 h) + S (5‘) + D (5′)	
Int.An-Ae SBR	13.0; 4.0	50	0.8	6–24	72.5 ± 23.3	ii	Dye-SWW (1270)			Total (24 h): F (15′) + An1* (8.9 h) + Ae1 (2.9 h) + An2* (8.9 h, RC) + Ae2 (2.9 h) + S (5′) + D (5′)	
Int.An-Ae SBR	15.3; 1.5	50	0.1–1.5	24	n.i.	iii	Sterilized RTWW (200–3000)	n.i.	n.i. (550–2000 ADMI)	Total (24 h): F (15′) + An1# (5.9 h) + Ae1 (5.9 h) + An2# (5.9 h) + Ae2 (5.9 h) + S (5′) + D (5′)	
An-Ae SBR	15.0; 1.0	50	2	24	n.i.	iii	Sterilized RTWW (800–1000)	n.i.	n.i. (1400–1800 ADMI)	gr.: Total (6 h): F (5′) + An (2.8 h) + Ae (2.8 h) + S (5′) + D (5′)	dec.: Total (24 h): F (n.i.) + An (18 h) + Ae (6 h) + S (n.i.) + D (n.i.)
SBBGR	n.i.; 14	n.i.	0.4–3.4	17–53	160	iv	RTWW (688 ± 280)	n.i.	Direct, disperse and reactive dyes	Total (6–8 h): F (n.i., up-flow through sludge bed) + Ae (n.i.; WW continuously aerated and recycled) + D (15′)	
SBBGR	n.i.; 9	n.i.	2	11	> 150	iv	30% RMWW + 70% RTWW (249 ± 65)	n.i.	n.i.	Total (6 h): F (15′, up-flow through sludge bed) + Ae (330′; WW continuously aerated and recycled) + D (15′)	
An-Ae SBR	17.1; 4.0	71	1	34.3	n.i.	iv	gr.-SWW dec.- 7% SWW + 93% RTWW (Ci: 1200)	Acetate	Mixture of textile dyes (Ci: 180 SU)	gr.: Total (6 h): F (4′) + An* (1 h) + Ae (4.8 h) + S (3–7′) + D (3′)	dec.: Total (24 h): F (n.d.) + An (18 h, N_2) + Ae (6 h)
gr.: Ae SBR dec.: BSR	27.3; 3.0	50	n.i.	n.i.	n.i.	v	gr.: SWW dec.: Dye-SWW (64000)	Peptone, Yeast extract	Reactive Blue 59 (5000)	gr.: Total (6 h): F (10′, static anoxic) + Ae (5.6 h) + S (5′) + D (10′)	dec.: Batch reactor, static anoxic conditions
gr.: Ae SBR dec.: BMR	n.i.; gr.: 3 dec.:1	70	n.i.	n.i.	n.i.	vi	Dye-SWW (TOC:16 mg L^{-1})	dec.: Lactate	Reactive Yellow 15 (5–50)	gr.: Total (6 h): F (60′) + Ae (4.5 h) + S (5′) + D (10′)	dec.: Microaerophilic batch tests**: 24 h for 80 days

Table 3 continued

System[a]	H/D; V (L)[b]	VER (%)[c]	OLR[d]	HRT (h)[e]	SRT (d)[f]	Seed[g]	WW type (COD)[h]	Substrate[i]	Dye (mg L^{-1})[j]	Cycle[k]
An-Ae SBR	4.0; 5.0	67	2.8	9	n.i.	iv	gr.: SWW dec.: Dye-SWW (700)	Acetate	Acid Red 18 (Ci: 50–100)	Total (6 h): F (4′) + An^{θ} (80′) + Ae (4.3 h) + S (5′) + D (1′)
I: An-Ae SBR II: Int.An-Ae SBR	2.5; 1.5	50	2	12	6–15	iv	Dye-SWW (1000)	Emsize E1	Acid Red 14 (40)	Total (6 h): F (15′) + An^{θ} [3.5 h (I) or 6 × 0.5 h (II)] + Ae [2 h (I) or 6 × 20 h (II)] + S (3–4′) + D (1′)
An-Ae SBR	2.5; 1.5	50	2–6	12	> 25	vii	Dye-SWW (1000–3000)	Emsize E1	Acid Red 14 (40–120)	Total (6 h): F (18′) + An^{θ} (1.5 h) + Ae (3.5 h) + S (5′) + D (1′)
An-Ae SBR with static (A) vs PF (B) feeding	2.5; 1.5	50	2–6	12	2–9 (A) vs 6–18 (B)	viii	Dye-SWW (1000–3000)	Emsize E1 and/or acetate	Acid Red 14 (40–120)	Total (6 h): F [30′ (A) vs 50–80′ (B)] + An^{θ} [1.5 h (A) vs 1.0–1.5 h (B)] + Ae (3.5 h) + S (5′) + D (1′)
Ae SBR	5.5; 4.0	n.i.	n.i.	n.i.	n.i.	ix	Dye-SWW (n.i.)	Glucose	Eriochrome Black T (50–400)	Total: 6 h [or 12–24 h for dye conc. > 200 mg L^{-1}]: F (10′) + Ae (4.5 h) + S (30′)
gr.: Ae SBR dec.: BSSR	27.3; 3.0	50	n.i.	n.i.	n.i.	x	gr.: SWW dec.: Dye-SWW (n.i.)	Peptone, Yeast extract	Reactive Blue 4 (Ci: 50–1000)	gr.: Total (6 h): F (10′, static anoxic) + Ae (5.6 h) + S (5′) + D (10′) / dec.: Batch reactor, static + shaking conditions
Anoxic-aerobic SBR	12.5; 4.0	50	n.i.	8	n.i.	xi	Dye-SWW (Ci: 500)	Glucose, acetate, etc.	Methylene Blue (4–10)	Total: 4 h F (3′) + Anoxic[#] (0.5 h) + Ae (3.3 h) + S (2′) + D (5′)

System[a]	Op.; Gr. (d)[l]	AG size (mm)[m]	SVI_{30} (mL g^{-1})[n]	Color (%)[o]	COD (%)[p]	NH_4-N (%)[q]	Aromatic amine formation and fate[r]	Reference
Int.An-Ae SBR	66; n.i.	2.3 ± 1.0 max.: 4	69	62	94	95	n.i.	Muda et al. (2010)
An-Ae SBR	72; 60	0.9 max.: 2.5	61	56	93	93	n.i.	Muda et al. (2012)
Int.An-Ae SBR	46 of 278; n.i.	0.6	15.5 ± 1.3	87	94	n.i.	n.i.	Muda et al. (2011)

Table 3 continued

System[a]	Op.; Gr. (d)[l]	AG size (mm)[m]	SVI_{30} (mL g^{-1})[n]	Color (%)[o]	COD (%)[p]	NH_4-N (%)[q]	Aromatic amine formation and fate[r]	Reference
Int.An-Ae SBR	42; 42	3–10	90–130	90	80	n.i.	n.i.	Ibrahim et al. (2010)
An-Ae SBR	112; 112	3.3 ± 0.9	35.1 ± 5.5	61	46	n.i.	n.i.	Kee et al. (2014)
SBBGR	200; n.i.	0.5	60–80	0–60	55–78	n.i.	n.i.	Lotito et al. (2012b)
SBBGR	200; 90	n.i.	n.i.	33.9 ± 8.0 41.9 ± 6.9 52.6 ± 9.8	82.1 ± 3.6	95.0 ± 7.4	n.i.	Lotito et al. (2014)
An-Ae SBR	187; 94	> 0.3 (80%) > 0.5 (50%)	70	73	68	n.i.	n.i.	Manavi et al. (2017)
gr.: Ae SBR dec.: BSR	60; 20	1–2	300	Complete after 8–12 h	56	n.i.	Formation of unidentified metabolites	Kolekar et al. (2012)
gr.: Ae SBR dec.: BMR	80; 45	1.2 ± 0.4	SVI_5: 38.4	89–100	79–95	92–100	n.i.	Sarvajith et al. (2018)
An-Ae SBR	75; 30	0.9–1.2	50	30–55	> 85	n.i.	No metabolite transformation	Moghaddam, Moghaddam (2016)
I: An-Ae SBR II: Int.An-Ae SBR	75; 30	0.5	67	80–85	80	n.i.	Formation of 4A1NS and unknown metabolites; No 4A1NS conversion	Mata et al. (2015)
An-Ae SBR	102; n.i.	0.3–1.0	17	> 90	80	n.i.	Formation of 4A1NS and unknown metabolites. Complete 4A1NS conversion after day 71	Franca et al. (2015)
An-Ae SBR with static (A) vs PF (B) feeding	315; n.i.	< 0.6 (E1) > 1.0 (Acetate)	54–310 (A) 51–179 (B)	66–91	68–90	n.i.	Formation of 4A1NS in and other unknown metabolites. No 4A1NS conversion	Franca et al. (2017)
Ae SBR	n.i.; 15	1.0–4.7	72	> 96	94	n.i.	n.i.	Hailei et al. (2010)
gr.: Ae SBR dec.: BSSR	n.i.; 180	7–9	n.i.	48–72 (after 48 h)	90 (after 72 h static)	n.i.	Maximal amines conc. after 48 h under static cond; 95%↓ under shaking	Chaudhari et al. (2017)

Table 3 continued

System[a]	Op.; Gr. (d)[l]	AG size (mm)[m]	SVI_{30} (mL g^{-1})[n]	Color (%)[o]	COD (%)[p]	NH_4-N (%)[q]	Aromatic amine formation and fate[r]	Reference
Anoxic-aerobic SBR	173; 87	2–4	43	56	93	n.i.	n.i.	Ma et al. (2011)

[a]Ae: aerobic; An: anaerobic; BMR: batch microaerophilic reactor; BSSR: batch static-shaking reactor; BSR: batch static reactor; dec.: decolorization experiment; gr.: granulation experiment; Int.: intermittent PF: plug-flow feeding through the sludge bed; SBBGR: sequencing batch biofilm granular reactor, composed by a microbial bed developed on plastic support material kept between two sieves (bottom of the reactor) and a liquid phase (top layer); SBR: sequencing batch reactor

[b]dec.: decolorization experiment; gr.: granulation experiment; H/D: height-to-diameter ratio of the reactor; n.i.: not indicated; V: volume of the reactor

[c]n.i.: not indicated; VER: volumetric exchange ratio

[d]n.i.: not indicated; OLR: organic loading rate (expressed as kg O_2 m^{-3} d^{-1})

[e]HRT: hydraulic retention time; n.i.: not indicated

[f]n.i.: not indicated; SRT: sludge retention time

[g](i) mixture of conventional activated sludge (CAS) from a municipal wastewater treatment plant (WWTP), CAS from textile mill WWTP, and anaerobic granules from an upflow anaerobic sludge blanket reactor treating paper mill industrial wastewater; (ii) aerobic granular sludge (AGS) developed according to Muda et al. 2010; (iii) sterilized sludge from a textile WWTP and an acclimatised mixed bacterial culture (*Alcaligenes* sp., *Bacillus* sp., *Acinetobacter* sp. and *Stenotrophomonas* sp.) added in every cycle filling stage; (iv) CAS from municipal WWTP; (v) isolates from soil/sludge contaminated with textile dye industrial wastewater; (vi) CAS with synthetic wastewater containing acetate (for the granulation experiment) or AGS acclimatized to the dye in 72 h cycle for 19 days (decolorization experiment); (vii) AGS from a municipal WWTP; (viii) stored AGS, previously acclimatized to Acid Red 14; (ix) CAS and micro-mycelium pellets from a white rot fungus; (x) bacterial cultures from a dye-contaminated area; (xi) CAS from a municipal WWTP, acclimatized to Methylene Blue

[h]Ci: initial substrate concentration in the reactor; COD: chemical oxygen demand (expressed as mg O_2 L^{-1}); dec.: decolorization experiment; dye-SWW: dye-laden synthetic wastewater; gr.: granulation experiment; n.i.: not indicated; RMWW: real municipal wastewater; RTWW: real textile wastewater; SWW: synthetic wastewater; TOC: total organic carbon; WW: wastewater. The COD values refer to the feed, except where Ci is indicated

[i]Emsize E1: hydrolyzed hydroxypropyl starch (commercial sizing agent, typically used in the cotton textile industry); etc.: starch, peptone, meat extract; dec.: decolorization experiment; n.i.: not indicated

[j]ADMI: American Dye Manufacturing Units; Mixture of dyes: Sumifix Black EXA, Sumifix Navy Blue EXF and Synozol Red K-4B; Ci: initial dye concentration in the reactor; n.i.: not indicated; SU: space units. The dye concentration values refer to the feed, except where Ci is indicated

[k] *Mixed liquor recirculation; #: static conditions; θ: mechanical mixing;': minutes; Ae: aerobic phase; An: anaerobic phase; D: drain phase; dec.: decolorization experiment; F: feeding phase; gr.: granulation experiment; N_2: sparging with nitrogen gas; n.i.: not indicated; S: settling phase. **: microaerophilic conditions imposed in loosely screw-capped bottles, incubated at 30 °C, 140 rpm in an orbital shaker; WW: wastewater

[l]Gr.: granulation period; n.i.: not indicated; Op.: operational period

[m]AG: aerobic granules; E1: Emsize E1 (hydrolyzed hydroxypropyl starch); max.: maximal size; n.i.: not indicated

[n]n.i.: not indicated; SVI_{30}: sludge volume index after 30 min of settling; SVI_5: sludge volume index after 5 min of settling

[o]Color removal yield

[p]Chemical oxygen demand (COD) removal yield

[q]NH_4-N: Ammonia–nitrogen removal yield; n.i.: not indicated

[r]↓: decrease; 4A1NS: 4-amino-naphthalene-1-sulfonic acid; conc.: concentration; n.i.: not indicated

In light of the low color removal efficiencies obtained (Muda et al. 2010, 2012; Table 3), Muda et al. (2011) optimized the treatment performance by selecting a hydraulic retention time (HRT) of 24 h and a long anaerobic phase; 3). The good AGS properties observed under these conditions indicated that the aerobic granular structure provided protection towards the presumably high concentrations of dyestuff degradation products (Muda et al. 2011).

In a similar SBR system (Ibrahim et al. 2010; Table 3), the same research group reported on the development of stable AGS, able to successfully remove COD and color from a real TWW Similarly to the previous studies, Kee et al. (2014) showed that best treatment performance was achieved when the HRT was increased to 24 h, using 24-h cycles with an 18-h anaerobic phase followed by a 6-h aerobic phase. Further increasing the HRT to 48 h led to a reduction in the color removal yield, possibly due to autoxidation of aromatic amine metabolites.

Sequencing batch biofilter granular reactor As an alternative aerobic, granular-based system, a sequencing batch biofilter granular reactor (SBBGR), comprising a sludge bed where biomass grew in the form of granules and biofilms (Lotito et al. 2012b; Table 3), was reported to meet the COD limit for discharge into the local sewer system, but the color removal yields were highly unstable due to the wide dye variability in the real TWW composition. Yet, although the treatment levels were insufficient for direct discharge into superficial water bodies, the treated wastewater was apparently allowed into the municipal sewer system (i.e., color not visible after a 40-fold dilution). Although the decolorization process (biodegradation and/or adsorption) was not investigated, the authors suggested that the high operating SRT could promote the development of species able to degrade dyes, and the presence of anoxic niches in the sludge could allow the reduction of dyes. Yet, the capacity of the system to effectively degrade azo dyes and to detoxify wastewater should be assessed in the future. The SBBGR sludge, described as a mixture of biofilm and (aerobic) granules packed in a filling material, was characterized in another study, revealing good settling and dewatering properties (Lotito et al. 2012a).

This system was further studied (Lotito et al. 2014) regarding the treatment of a mixed municipal-TWW, corresponding to the influent of a biological reactor in a WWTP. The good COD, nitrogen, TSS and surfactants removal yields, as well as the partial color removal yields (Table 3) achieved by the SBBGR system alone, complied with the local limits for direct discharge (i.e., color not visible after a 20-fold dilution). Comparing with a conventional WWTP (secondary and tertiary treatments, including biological treatment, coagulation-flocculation and ozonation), the SBBGR system produced an effluent of comparable quality using a simpler treatment scheme, with lower HRT (11 h vs 30 h) and sludge production, which further supported the application of this aerobic, granular-based system as a main treatment unit at WWTPs treating mixed municipal-TWW (Lotito et al. 2014). Furthermore, microbial community analysis indicated that *Betaproteobacteria* represented more than 40% of the biomass, *Actinobacteria* and *Alphaproteobacteria* being other relevant groups in the SBBGR. In addition, the presence of nitrifying and denitrifying bacteria was confirmed, corresponding to approximately 3% and 6% of active bacteria in the bioreactor, respectively (Lotito et al. 2014).

Anaerobic–aerobic SBR More recently, Manavi et al. (2017) reported color and COD removal yields around 70%in an anaerobic–aerobic AGS SBR after gradual adaptation of the mature AG to real dyeing wastewater (Table 3). In addition, some color formation during the aerobic phase was hypothetically attributed to the autoxidation of the dye reduction metabolites. On the other hand, color removal during the aerobic phase was registered when AG with sizes above 0.3 mm represented more than half of the biomass. In this context, the authors considered the possible partial contribution of dye biosorption to the surface of AG, but also suggested the occurrence of azo dye reduction inside AG during the aerobic phase, which was further supported by the presence of cavities within the tightly linked bacterial structure, potentially serving as channels for movement of dyes and metabolic products within AG. Owing to the high variability in TWW, and the limitation of the color removal yield to 73% reported in this study, the authors suggested that in addition to further optimization of the SBR operational conditions, implementation of a subsequent physicochemical treatment might be necessary for decolorizing textile dyes of types other than azo dyes, which are presumably recalcitrant under these operational conditions. Regarding AG stability, exposure of AGS to the increasing

concentration of the real dyeing wastewater, concomitantly with the extension of the anaerobic-to-aerobic phase duration ratio and HRT, enhanced EPS production but reduced the granular mass fraction in the sludge, which indicated the occurrence of AG disintegration along SBR operation. In this sense, the authors highlighted that further assessment of the AG instability during long-term operation with real dyeing wastewater is needed before this technology can be considered for this application.

The use of real TWW (Ibrahim et al. 2010; Kee et al. 2014; Lotito et al. 2012b, 2014; Manavi et al. 2017) or synthetic TWW containing a mixture of several textile dyes (Muda et al. 2010, 2011, 2012) better mimics the complexity of real environmental conditions, which is essential to evaluate the potential for AGS application to TWW treatment. However, optimization of AGS SBR systems specifically towards an efficient decolorization performance and analysis of the underlying mechanisms requires the use of simpler feed wastewater compositions. In this sense, the subsequently reviewed AGS studies focused on decolorization by employing simulated TWW containing only one textile dye.

2.2.3.3 Synthetic TWW containing one azo dye **Anoxic and microaerophilic batch tests** Through the use of batch decolorization tests, Kolekar et al. (2012) showed that AG were able to completely decolorize up to 5 g L^{-1} of Reactive Blue 59 through azo bond reduction, as confirmed by the disappearance of the azo dye peak in HPLC chromatograms and emergence of new, unidentified peaks at higher RTs. The azo dye biotransformation products presented no genotoxicity, as opposed to the parental dye, but the COD removal yield decreased with increasing initial dye concentrations. In addition, induction of azo reductase and cytochrome p450 levels in the dye decolorizing AGS suggested their involvement in biodecolorization. Finally, although exposure to this high azo dye concentration was associated to significant changes in the microbial community (except for the unaffected *Acidobacteria* phylum), the azo dye decolorizing AGS were characterized by a diverse microbial community belonging to *Alpha-*, *Beta-*, and *Gamma-proteobacteria* (Kolekar et al. 2012).

Similarly, a recent study (Sarvajith et al. 2018; Table 3) reported that AGS was able to effectively decolorize Reactive Yellow 15, stable and high azo dye, total organic carbon, ammonia and total nitrogen removal yields being achieved under microaerophilic conditions (DO within 0.1–2.0 mg L^{-1}). Furthermore, this work confirmed that azo dye biodecolorization and ammonia removal via the nitrite pathway occurred simultaneously under microaerophilic conditions, which is advantageous over the conventional nitrification–denitrification process in terms of oxygen and COD requirements (Sarvajith et al. 2018). In this sense, the authors suggested that AGS operation under microaerophilic conditions is promising for treating dye-laden TWW either onsite in textile industries or after dilution with domestic sewage.

Specifically regarding color removal, Sarvajith et al. (2018) showed that Reactive Yellow 15 adsorbed to the AG when a carbon source was absent, but this was revealed to be a reversible and unstable process. On the other hand, the azo dye was sustainably decolorized in the presence of lactate and at DO values lower than 0.5 mg L^{-1}. Although the microaerophilic conditions might allow both reductive and oxidative reactions, thus potentially leading to complete azo dye biodegradation, HPLC analysis was unsuccessful in identifying biotransformation intermediates (Sarvajith et al. 2018). Moreover, the presented general absorbance decrease in the UV–visible spectra (300–800 nm) and lack of information regarding the absorbance profile in the wavelength range below 300 nm, provided insufficient evidence to conclude about the biodecolorization mechanism, thus requiring further analysis. Nevertheless, the authors proposed a metabolic pathway depicting lactate, azo dye and ammonia–nitrogen (NH_4–N) removal processes in an AGS system, where lactate acted as source of reducing equivalents for both azo dye and nitrite reduction.

Finally, this study showed that AGS recovered good settling properties after initial granule break-up due to changes in operational conditions (i.e., switch in the carbon source from acetate to lactate, as well as exposure to the azo dye and low DO), which also induced a shift in the AGS bacterial community (Sarvajith et al. 2018). Specifically, while acetate-fermenting bacteria were eliminated, the bacterial community became enriched in specific microorganisms previously associated with azo dye decolorization (e.g., laccase producing *Streptomyces* sp., *Vagococcus* sp., *Enterococcus* sp., *Bacillus* sp., *Brevibacillus* sp., and *Staphylococcus* sp., as well as

Rhodococcus sp. and *Stenotrophomonas* sp.). Likewise, comammox microorganisms, namely *Nitrospirae*, were detected in the Reactive Yellow 15-decolorizing AGS.

Mechanically stirred anaerobic–aerobic SBR According to Moghaddam and Moghaddam (2016; Table 3), mature AGS removed more than 85% of COD and around 54% of color deriving from Acid Red 18 in an anaerobic–aerobic SBR. Similarly to Manavi et al. (2017), despite the fact that most of the decolorization occurred during the anaerobic phase, presumably through azo bond reduction, significant color removal was further registered during the aerobic phase, its contribution (ca. 25%) to the overall color removal yield increasing when larger AG were observed, potentially providing larger anaerobic cores (Moghaddam and Moghaddam 2016). Moreover, the contribution of dye adsorption onto AGS for decolorization was insignificant (less than 8%). In this sense, Moghaddam and Moghaddam (2016) hypothesized that Acid Red 18 could reach the AG inner layers, where anaerobic microorganisms performed azo dye reduction during the aerobic phase (DO in the range of 5–6 mg L^{-1}; oxidation–reduction potential around +150 mV), coupled with the use of tightly bound-EPS (TB-EPS) as carbon and energy source. On the other hand, UV–visible spectra analysis (200–900 nm) revealed that the AGS was unable to further aerobically degrade the intermediates produced from Acid Red 18 reduction (namely the recalcitrant aromatic amine 4A1NS). While the developed granules presented a stable and compact structure in the treatment of synthetic wastewater containing 50 mg L^{-1} of azo dye, AG disintegration occurred when the dye concentration was doubled and the system's color removal yield deteriorated to 30% (Moghaddam and Moghaddam 2016). In addition to the AG instability, the decreased color removal efficiency was attributed to the presence of excess loosely bound-EPS (LB-EPS) on the surface of AG resulting from the azo dye shock load, possibly leading to AG pore clogging and consequently to reduced dye penetration and decolorization in the AG inner zones.

Overall, despite the well described presence of anaerobic and anoxic regions within AG (Winkler et al. 2013), color removal by AGS under aerobic conditions has only been significantly observed in few studies, though in relatively low extents when compared to the removal yields registered under anaerobic conditions (Manavi et al. 2017; Moghaddam and Moghaddam 2016; Muda et al. 2010). Moreover, none of these studies confirmed (e.g., by HPLC) that the observed aerobic decolorization effectively resulted from azo bond reduction occurring in the anaerobic core of AG during the aerobic phase, which would imply that azo dyes diffused into the AG center. In fact, color removal has mainly been reported during the anaerobic phase, indicating that the use of combined anaerobic–aerobic AGS processes is more appropriate for the treatment of dye-laden TWW. In this sense, most of the studies addressing this particular application also included an anaerobic phase during initial AGS formation, irrespective of the presence of dyes during this period (Table 3). However, the majority of the studies investigating granulation and AGS system performance have been conducted in aerobic or anoxic-aerobic cycles (Franca et al. 2018). Therefore, there is comparably less information regarding the development and especially the long-term stability of AG under anaerobic–aerobic cycles, which requires further study (Manavi et al. 2017). This is especially relevant when mechanical stirring is used during the anaerobic phase. Most of the studies previously reviewed promoted anaerobic conditions either through liquid recirculation (Muda et al. 2010, 2011), static conditions (Ibrahim et al. 2010; Kolekar et al. 2012) or nitrogen gas sparging (Manavi et al. 2017). As further reviewed, in addition to Moghaddam and Moghaddam (2016), a mechanically stirred anaerobic phase to promote azo dye reduction was only employed by another research group (Franca et al. 2015, 2017; Lourenço et al. 2015; Mata et al. 2015), which operated SBRs with the lowest reported height-to-diameter ratio (H/D = 2.5; non-tubular reactors), representing a potential advantage in terms of full-scale implementation.

Mata et al. (2015) were the first to report the use of a stirred anaerobic–aerobic, non-tubular SBR for the development and operation of AGS in the treatment of a synthetic TWW (Table 3). The granulation period was similar to those of most of the literature studies employing tubular SBRs, but the produced AG were smaller (Table 3), possibly due to lower selective pressure (H/D = 2.5) and higher shear stress (mechanical stirring). In addition, better granulation was achieved in the presence of Acid Red 14, in comparison to a dye-free control. High overall color and COD removal yields were achieved under two 6-h

sequencing batch cycle strategies (Table 3), but higher initial decolorization rates were obtained using in a single anaerobic–aerobic reaction phase. HPLC analysis proved that decolorization was a result of complete azo bond reduction, producing a stable aromatic amine (4A1NS) in stoichiometric amounts, which was not aerobically degraded, similarly to another study (Moghaddam and Moghaddam 2016). Finally, Mata et al. (2015) suggested that prolonging the aerobic phase (and consequently the exposure to shear stress and the famine period) could possibly further improve granulation and COD removal performance.

In light of AGS application to treat real TWW, Manavi et al. (2017) raised the question of whether AG should be developed in wastewater containing no dyes, with the advantage of granulation not being adversely affected by them or other potentially toxic components, or whether it should occur in dye-containing wastewater, in which case the microbial community within AG would adapt sooner to the TWW components and potentially perform better in its treatment. Overall, formation of AGS has been successfully performed using uncolored synthetic wastewater (Chaudhari et al. 2017; Manavi et al. 2017; Moghaddam and Moghaddam 2016), dye-laden textile synthetic wastewater (Kolekar et al. 2012; Mata et al. 2015; Muda et al. 2010, 2012) and real TWW (Ibrahim et al. 2010; Kee et al. 2014), with varying granulation times (20–180 days, 30–87 days and 42–112 days, respectively). Furthermore, Franca et al. (2015) used mature AGS, previously developed with real wastewater in a municipal WWTP (Frielas WWTP, Portugal), as inoculum for treating a synthetic TWW in a lab-scale SBR.

Following the study of Mata et al. (2015), Franca et al. (2015) studied the effect of Acid Red 14 on the performance of an anaerobic–aerobic AGS SBR system (Table 3). High shear stress caused by mechanical stirring resulted in initial disintegration of the large AG used as inoculum (with sizes up to 5 mm, harvested from a bioreactor treating domestic wastewater) giving rise to small, compact granules (sizes up to 1 mm) with excellent settling properties (Table 3). Overall, the dye and its breakdown products negatively affected neither biomass growth in the reactors nor treatment performance, as COD removal yields higher than 80% were attained in both the dye-free (control) and dye-fed reactors after 14 days of operation. Moreover, up to 77% of COD removal was registered during the anaerobic phase, being correlated with an increase in the abundance of *Defluviicoccus vanus*-related glycogen-accumulating organisms (GAO), known to be able to take up saccharides anaerobically. The decrease in the anaerobic-to-aerobic phase time ratio, when compared to the previous work (Mata et al. 2015; Table 3), allowed the complete bioconversion of the aromatic amine (4A1NS), identified as primary dye reduction product, along the aerobic reaction phase (when the SRT was above 25 days), without compromising the high color removal efficiency during the anaerobic phase. Yet, the stable dye reduction yields (above 90%, reached after 11 days of operation) suffered a 30% reduction during a 2-week period, when daily biomass harvesting was conducted to control the SRT at 15 days. These results highlighted the importance of SRT control flexibility in AGS systems for the development of a more diverse microbial population with the ability to remove color through azo bond reduction and to further mineralize the resulting aromatic amines. Finally, the capacity of the system to deal with shocks of high dye concentration and organic load in the feed was successfully demonstrated, as granule stability, high color and COD removal yields were sustained (Franca et al. 2015), in contrast with a previously mentioned study (Moghaddam and Moghaddam 2016).

By comparing the anaerobic–aerobic AGS SBR system described by Franca et al. (2015) with an anaerobic–aerobic CAS SBR treating the same wastewater, Lourenço et al. (2015) reported that similar color removal yields (75–80%) were attained in the two systems but with higher anaerobic and overall COD removal yields in the AGS SBR. The superior AGS performance is possibly related with the protective effect provided by the granular structure, alleviating the apparent inhibitory effect of the azo dye towards the organic load removal by CAS. In addition, detoxification of the wastewater was only observed during the aerobic reaction phase in the AGS SBR system (after 70 days of operation), where at least one of the azo dye metabolites (4A1NS) was aerobically biotransformed (Franca et al. 2015), as opposed to the CAS SBR, where the same metabolite remained unconverted (Lourenço et al. 2015). These findings further highlighted the better performance of the AGS system comparatively to conventional anaerobic–

aerobic SBR technology based on floc-forming bacteria. Overall, according to this comparative study, the three main practical factors supporting the application of the AGS technology for TWW treatment in replacement of flocculent biomass SBR are as follows (Lourenço et al. 2015): (1) the excellent settling properties of AGS allow shorter SBR cycles with similar color removal and higher COD removal yields; (2) the granular structure increases the tolerance to toxicity and to high organic loads; (3) the excellent biomass retention of AGS systems allows bioreactor operation at higher SRT values, possibly favoring the establishment of a more diverse microbial population with the potential ability to biodegrade recalcitrant aromatic compounds such as aromatic amines.

In terms of stability, Franca et al. (2015) also reported that granule break-up after long-term operation only occurred in a dye-free control SBR, and not in a dye-fed SBR operated alongside it. The authors suggested that the azo dye may play a role in improving AG stability by acting as electron acceptor and thus promoting heterotrophic growth in the anaerobic core of AG. In fact, fluorescence in situ hybridization (FISH) analysis confirmed the compact structure of the dye-fed AG, microbial activity being apparently maintained in the granule core, as opposed to the dye-free control (Franca et al. 2015). As highlighted by Manavi et al. (2017), stability of AG during long-term exposure to dye-containing wastewaters is an important issue that deserves further investigation, as well as the AG disintegration effect associated with the presence of high azo dye concentrations (Moghaddam and Moghaddam 2016). In this context, Franca et al. (2017) compared two feeding strategies regarding the capacity of anaerobic–aerobic SBRs to deal with disturbances in the composition of a simulated TWW containing the azo dye Acid Red 14 (Table 3). Both a statically fed, anaerobic–aerobic SBR and an anaerobic plug-flow fed, anaerobic–aerobic SBR (where the biomass contacted more thoroughly with the feed during the fill stage) could cope with shocks of high azo dye concentration and organic load, the overall COD and color removal yields being rapidly restored to 80%. Yet, the shock loads had a negative effect on AG integrity and aerobic bioconversion of the amine metabolite (4A1NS) was not observed along the 315-day run. Switching from a hydrolyzed starch based to an acetate based feed deteriorated AGS stability. In addition, although COD uptake was minimal in the plug-flow feeding stage, the fraction of COD removed anaerobically was generally higher in the plug-flow fed SBR. Overall, the latter recovered more rapidly from the imposed disturbances, revealing a higher capacity to deal with substrate-related variations. These results further highlighted the need for more research to ensure long-term AGS stability during the treatment of azo dye-laden TWW.

Aerobic SBR Differently from the aforementioned studies, Hailei et al. (2010) developed AG bioaugmented with a specific fungal strain (white rot fungus *Phanerochaete* sp. HSD) able to form micro-mycelium pellets and to degrade azo dyes using its manganese peroxidase system (Table 3). Specifically, by seeding an aerobic SBR with micro-mycelium pellets and CAS, granulation was achieved faster than in an SBR seeded only with CAS, probably because the small pellets served as primary matrices acting as nuclei for initial AG formation (Hailei et al. 2010). However, 92% of the analyzed mature AG did not have a micro-mycelium pellet as nucleus. In terms of treatment performance, the bioaugmented AG presented a higher tolerance and decolorization efficiency towards the azo dye (Eriochrome Black T)-laden synthetic TWW, when compared to CAS and conventional AG under the employed operational conditions (aerobic reaction). Since the contribution of adsorption was not relevant at the tested dye concentrations (Table 3), the authors proposed that the bioaugmented AG probably removed the dye Eriochrome Black T through azo bond cleavage and further degradation of the generated aromatic amines by manganese peroxidase, the activity of which was detected in the SBR.

2.2.3.4 TWW containing one non-azo dye In addition to azo dyes, which are the most prevalent class of dyes used by the textile industry, AGS has also been studied regarding the decolorization of other types of dyes. For instance, Chaudhari et al. (2017) showed that AGS was able to effectively decolorize an anthraquinone dye at concentrations up to 1 g L^{-1} (Table 3), mainly via initial reductive conversion, producing non-toxic metabolites. Specifically, results indicated that AGS effectively removed halogenated and amino groups from the dye, a Reactive Blue 4 biotransformation pathway by AGS being suggested (Chaudhari et al. 2017). Regarding the microbial community in AGS, exposure to Reactive Blue 4

promoted the presence of several groups, among which *Proteobacteria* (*Alpha*-, *Beta*-and *Gamma*-), *Firmicutes* and *Bacteroidetes* were highlighted for being able to tolerate the dye and for potentially being involved in its degradation (Chaudhari et al. 2017). These results supported the potential application of AGS for biotransformation and detoxification of the recalcitrant anthraquinone dye Reactive Blue 4.

In a previous study (Ma et al. 2011), AGS was successfully developed in an anoxic-aerobic SBR fed with a synthetic wastewater containing a cationic dye (Methylene Blue; Table 3), which was decolorized during the anaerobic and aerobic phases, with very low contribution from dye adsorption onto AG. In this context, the authors suggested the use of AGS technology for the pre-treatment of industrial wastewater containing Methylene Blue.

2.2.3.5 Dye removal through adsorption onto AGS Among the literature regarding the use of AGS for the treatment of TWW, some works were specifically focused on the removal of textile dyes through adsorption onto AG. Overall, researchers have explored the opportunity for using excess AGS produced during wastewater treatment as cheap sorbents for removing contaminants from wastewater (Nancharaiah and Reddy 2018). As previously reviewed (Adav et al. 2008), post-separation from the treated water, stability of biosorbents and regeneration after use are some of the drawbacks that limit the application of suspended adsorbents for the removal of dyestuffs from industrial wastewater. On the other hand, the high surface area, porosity and good settling properties of AG are attractive characteristics for removal of dyes and metals from wastewater through biosorption (Adav et al. 2008). In fact, AG have been rated with a three-fold higher maximum adsorption density than sludge flocs, regarding the cationic dye Rhodamine B (Zheng et al. 2005). Accordingly, Gao et al. (2010a) concluded that inactive (non-living) AGS could be effectively used as a low-cost, alternative biosorbent for the removal of Acid Yellow 17 dye from wastewater. The same authors also studied the competitive biosorption of Yellow 2G and Reactive Brilliant Red K-2G onto inactive AG, indicating that amine, hydroxyl and carboxyl groups were the main functional groups involved in biosorption of these dyes (Gao et al. 2010b). More recently, other studies successfully demonstrated the use of inactive AGS in the adsorption of Sunset Yellow FCF (Zhang et al. 2016b), Methylene Blue (Wei et al. 2015), Methyl Orange and Crystal Violet (Huang et al. 2018). Furthermore, Wei et al. (2015) distinguished between the contributions of EPS and sludge in the adsorption of Methylene Blue onto AGS, corresponding to 9.4% and 80.7%, respectively, of the overall effect. In addition to AGS biosorption, the same research group also analyzed the use of acid TiO_2 hydrosol as self-cleaning eluent for biosorbent recovery and photocatalytic dye degradation (Huang et al. 2018), the results supporting the combination of AGS biosorption and photocatalysis for dye-containing wastewater treatment.

2.2.3.6 Full-scale application Overall, the reported studies support the use of AGS in the treatment of dye-laden TWW, further research being necessary to achieve maximal and consistent biodecolorization and detoxification of these wastewaters before the scaling up of this specific application. Most of these studies were still done at laboratory scale and used synthetic wastewaters, reports on pilot-scale and full-scale implementation of anaerobic–aerobic AGS SBRs being still scarce. Li et al. (2014) reported that the full-scale AGS SBR at Yancang WWTP (China) treating a wastewater composed of 30% sewage and 70% industrial wastewater from printing, dyeing, chemical, textile and beverage industries exhibited excellent performance in terms of COD and NH_4-N removal, but color removal was not assessed. In addition, AG remained stable during long-term operation (Li et al. 2014), denoting the resistance of AGS to the toxic nature of these wastewaters. Furthermore, microbial community analysis of mature and stable AGS collected from a WWTP treating the same type of wastewaters (Haining, China) indicated that AGS was primarily composed of *Planctomycetes*, *Proteobacteria* and *Bacteroidetes* (Liu et al. 2017). *Euryarchaeota* phylum was found to constitute the majority of the archaea in AG while, more specifically, *Methanosaeta* genus was dominant in flocs. The higher diversity of bacteria and archaea in AG (vs the higher diversity of fungi in flocs) suggested that bacteria and archaeal microorganisms uniquely associated to AG may play a key role in their structure formation and stability, being maintained in the

system by the long SRT values employed (Liu et al. 2017).

3 Engineered nanoparticles (ENP) in the textile industry

3.1 Application and environmental concerns

Application of ENP in woven and non-woven textiles (e.g., rainwear, protective clothing, sportswear and automobile interior fabrics) represents one of the fastest developing process branches. The textile industry has recognized the excellent characteristics that ENP confer to textile materials, such as antimicrobial and protective properties, enhanced stain and water resistance, as well as increased ability to absorb dyes and change wettability (Rezić 2011).

The widespread and growing application of ENP in commercial products, namely in textile goods, has recently raised awareness regarding the implication of the likely high ENP concentration in the environment and its impact on human health (Brar et al. 2010). In fact, the release of ENP into the environment may occur during their synthesis, their incorporation into products, during the use of these goods and, finally, upon their recycling or disposal (Rezić 2011; Fig. 1). According to Rezić (2011), the most important sources

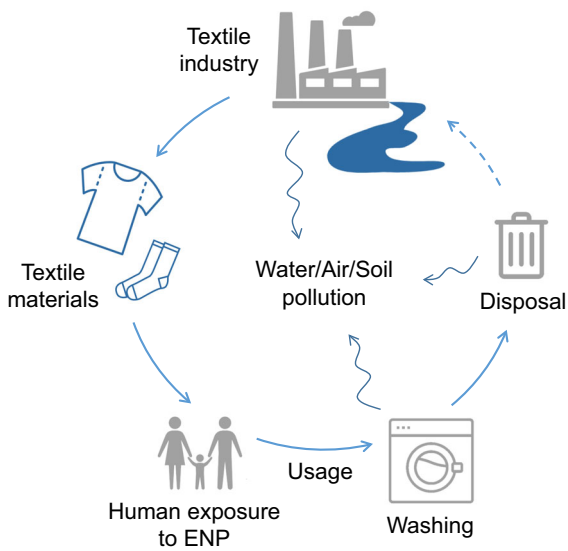

Fig. 1 Release of engineered nanoparticles (ENP) from textile materials into the environment throughout their life cycle

of textile ENP released to the environment are considered to be textile industry wastewaters and waters from large hospital or hotel laundries. The ENP pathway in a wastewater treatment plant (WWTP) depends on the physiochemical properties of the ENP, and their residence times in the different WWTP compartments, as well as on characteristics of the wastewater (namely, pH and suspended solids content) and its sludge (Brar et al. 2010). The subsequent fate of these contaminants can either be associated with the sewage sludge, potentially affecting soil ecosystems upon land application and incineration, or with the discharged water, eventually compromising life in aquatic ecosystems (Brar et al. 2010). Due to the potential long-term contamination of the aquatic and soil ecosystems with ENP if these escape from WWTPs, an understanding of the presence, behavior, fate and impact of ENP in wastewater and wastewater sludge along their treatment systems is urgently needed (Brar et al. 2010).

3.2 Silver nanoparticles (AgNP)

3.2.1 Characteristics and antimicrobial mechanisms

AgNP have been the most commonly used nanomaterial in consumer products (from antibacterial socks and nasal/throat sprays to beauty creams, toothpastes and vacuum cleaners), being one of the fastest-growing product categories in these industrial sectors (Sheng and Liu. 2017; Zhang et al. 2016a). Globally, the amount of AgNP applied in textiles has been estimated as 36 tons (Windler et al. 2013). Specifically, AgNP, clusters of zero-valent silver (Ag^0) with at least one dimension within the 1–100 nm range, provide antimicrobial and antibacterial characteristics to textiles, which is especially advantageous for medical, healthcare, hygiene and sports applications (Zhang et al. 2016a). Several antimicrobial agents have been used by the textile industry in antimicrobial finishing processes, such as metal salts and peroxy-acids, in order to minimize microbial growth on textiles and its associated negative effects (namely, unpleasant odor, stains, decolorization and contamination). However, AgNP, as well as other ENP (TiO_2 and CuO), have presented superior antimicrobial action in terms of efficiency and durability (Radetić 2013).

The strong antimicrobial activity of AgNP is non-specific, covering a broad range of microorganisms even at concentrations below 1 mg AgNP L^{-1} (Zhang et al. 2016a). The toxicity of nanoparticles varies with their physicochemical properties, namely surface characteristics (area, porosity, charge, surface modification and coating), size, shape, composition, chemical structure, and reactivity, being also dependent on several environmental conditions, such as pH, ionic strength and light (Rezić 2011).

Depending on the degree of Ag^+ release from AgNP, the toxicity of AgNP can be derived from the toxicity mechanisms of silver ions (Ag^+; ion-related toxicity) and/or silver particles (AgNP; particle-related toxicity), their respective contribution for the overall toxicity being still under debate (Sheng and Liu 2017). Yet, the release of Ag^+ from AgNP is generally regarded as the main toxicity effector (Fabrega et al. 2009; Peretyazhko et al. 2014; Zhang et al. 2016a, 2018a), and occurs in aqueous solution under oxic conditions, through a dissolution reaction where DO acts as an oxidant to produce a soluble silver oxide (Huangfu et al. 2019).

Owing to its high affinity for sulfur and phosphorus compounds, the ion-related toxicity generally involves Ag^+ binding to proteins, peptides and/or DNA, leading to enzyme deactivation, membrane permeability disruption and accumulation of intracellular radicals, resulting in microbial growth inhibition, cell death and lysis (Huangfu et al. 2019; Zhang et al. 2018a).

Regarding the particle-related toxicity mechanism, AgNP have been shown to enter the cell, where, similarly to Ag^+, Ag^0 at the surface of AgNP potentially interacts with proteins and DNA molecules, consequently disrupting key metabolic processes. The cell internalization process of AgNP can occur through direct penetration of the cell membrane (nonspecific binding), resulting in direct physical damage (Huangfu et al. 2019), or endocytosis through specific receptor-ligand interactions (Nel et al. 2009).

In this context, the toxicity of AgNP results from the combined effects of three interconnected toxicity pathways involving (1) the release and uptake of Ag^+ with consequent cellular enzyme deactivation, (2) the generation of reactive oxygen species (ROS; oxidative stress-related toxicity mechanism) on the surface of the AgNP or by the action of Ag^+, (3) cell membrane damage and permeability disruption inflicted directly by AgNP or indirectly by Ag^+ (Sheng and Liu 2017). Further investigations are required to fully understand the toxic mechanisms of AgNP (Zhang et al. 2018a).

3.2.2 *Fate of AgNP in wastewater treatment plants (WWTPs)*

An increased amount of AgNP is expected to be released into domestic and industrial waste streams due to its extensive application in consumer products (Hoque et al. 2012; Sheng et al. 2018). In general, studies suggest that the majority of AgNP in consumer products will reach WWTPs, which represent important barriers to prevent nanoparticles from directly entering the environment (Blaser et al. 2008). Accordingly, Zhang et al. (2016a) indicated that AgNP concentrations the influent of full-scale municipal and industrial WWTPs are generally in the μg L^{-1} order of magnitude (up to 15 and 193 μg L^{-1} total silver, respectively).

The various possible AgNP transformation pathways under the complex conditions present in real water environments make it difficult to assess their fate in WWTPs, and consequent environmental risk. The transformations that ENP generally undergo in aqueous environments include oxidation, dissolution, adsorption, aggregation and sedimentation. Specifically, Zhang et al. (2018a) reviewed four major chemical environmental AgNP transformations (oxidative dissolution, photoreduction, sulfidation and chlorination) that impact the fate and toxicity of AgNP under aqueous conditions. Recently, Huangfu et al. (2019) reviewed the possible interactions between ENP and microbial cells. Accordingly, Fig. 2 schematically summarizes the different chemical, physical and biological processes involved in the interaction between AgNP and microbial cells in a biological wastewater treatment system, as subsequently explained on the basis of the literature assessing AgNP fate in WWTPs.

As previously stated, the bactericidal activity of AgNP is in a major part attributable to the release of Ag^+ through oxidative dissolution under oxygen-rich aqueous conditions, depending on the DO and pH (oxidative dissolution is hindered under anoxic or alkaline conditions). In oxic water solutions, the oxidation of AgNP surfaces by O_2 or H_2O_2 to generate Ag_2O is a slow and rate-determining step for the subsequent, relatively quick dissolution of Ag_2O

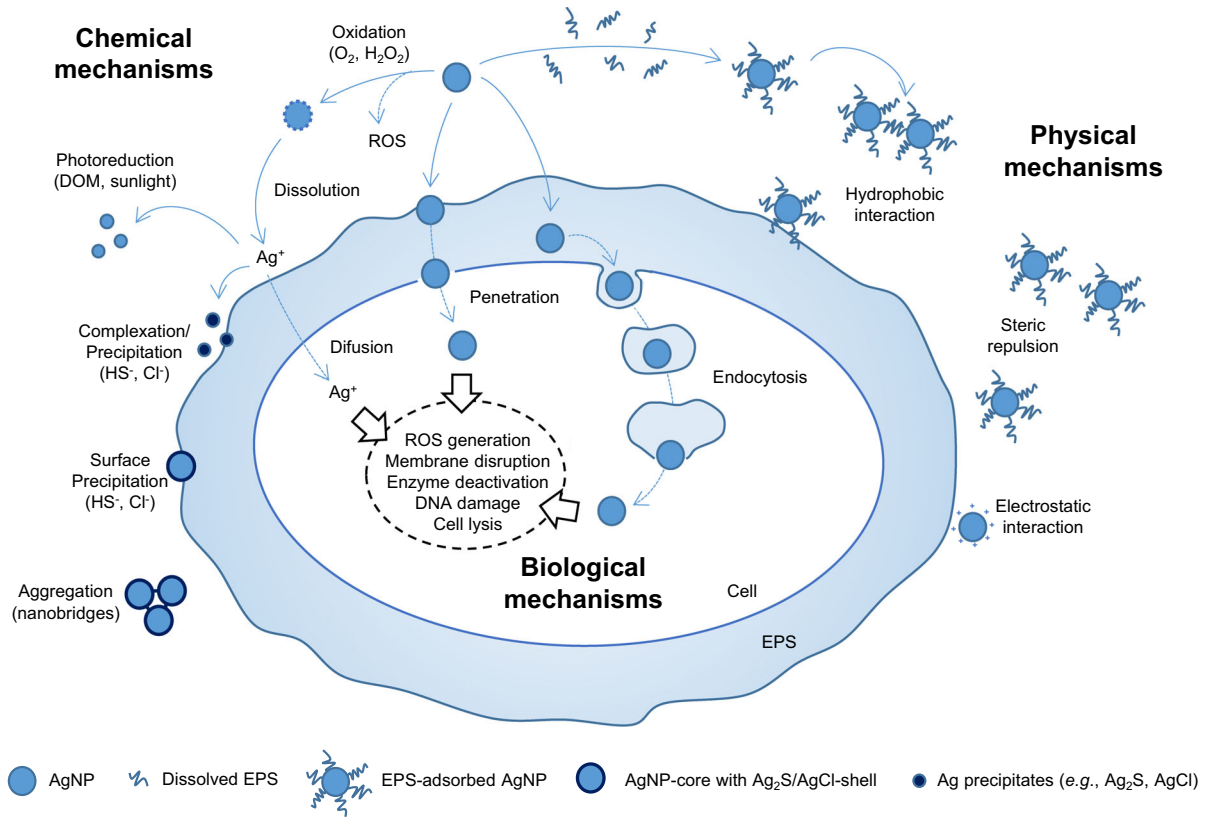

Fig. 2 Chemical, physical and biological mechanisms involved in the interaction between silver nanoparticles (AgNP) and microbial cells. *DOM* dissolved organic matter, *EPS* extracellular polymeric substances, *ROS* reactive oxygen species

(Fig. 2). Moreover, as the formed Ag_2O can adhere to the AgNP surface forming a Ag_2O shell surrounding a AgNP core, it can protect AgNP from further oxidation and decrease the surface available for dissolution. On the other hand, dissolved Ag^+ can be reduced by dissolved organic matter (such as phenol, quinone, ketone and hydroxyl groups) to form AgNP under (simulated) sunlight irradiation, through photoreduction (Yu et al. 2016; Fig. 2). Therefore, oxidative dissolution of AgNP and photoreduction of Ag^+ will occur simultaneously, reaching a dynamic equilibrium (Peretyazhko et al. 2014).

The natural presence of sulfur in aqueous environments allows the direct or indirect sulfidation of AgNP, owing to the high affinity of AgNP and Ag^+ towards sulfur (Fig. 2). Specifically, the high sulfide concentrations present in anaerobic environments typically allow the direct transformation of AgNP into Ag_2S nanoparticles (direct sulfidation). On the other hand, under low sulfide concentrations, Ag^+ previously formed from AgNP oxidative dissolution can rapidly precipitate with sulfide (indirect sulfidation), the formation of Ag^+ being the rate-determining step. Owing to the fact that Ag_2S nanoparticles are thermodynamically more stable than AgNP and that Ag_2S can block the surface of AgNP, sulfidation decreases the overall concentration of free Ag^+, diminishing the associated toxicity level (Zhang et al. 2018a). Moreover, Ag_2S precipitated on the AgNP surface has been shown to form Ag_2S nanobridges, linking neighboring AgNP, thus contributing to AgNP aggregation (Levard et al. 2012; Fig. 2).

Although AgNP are mainly reprecipitated as Ag_2S, indirect chlorination of AgNP can occur in seawater or chloride-rich water as Ag^+ resulting from AgNP oxidative dissolution precipitates in the form of AgCl (Fig. 2). Although sulfidation and chlorination can generally mitigate the toxicity of AgNP by decreasing the availability of Ag^+ species and their release from AgNP, the transformation products (Ag_2S and AgCl) are still bioavailable and toxic to some organisms, and

have high stability, resulting in long-term persistence in the environment (Zhang et al. 2018a). Similarly, the reaction of Ag^+ with phosphate or simple, common organic molecules relevant in aqueous environmental media (e.g., glucose or soluble microbial products) has been found to have a decelerating effect on AgNP dissolution (Loza et al. 2014). These environmental transformations of AgNP progress simultaneously in complex aquatic environments. Yet, the oxidative dissolution of AgNP represents a primary step for most of the other chemical processes (except for direct sulfidation), the DO playing a vital role in AgNP transformations.

Effective AgNP toxicity in the biological unit of a WWTP is dependent on the AgNP transformations occurring during transport through sewage networks and inside the bioreactor (Zhang et al. 2016a). Kaegi et al. (2013) showed that AgNP are transported in sewer systems without substantial losses to the sewer biofilm, the extent of AgNP sulfidation strongly depending on the AgNP size and on sulfide availability. Moreover, the vast majority of the AgNP were retained in the activated sludge flocs by heteroaggregation, irrespective of AgNP size and coating. In this sense, the authors suggested that measures to reduce TSS in the effluent should be implemented in order to avoid the associated AgNP escape from the WWTP (Kaegi et al. 2013).

The retention of AgNP in activated sludge has been associated to extracellular polymeric substances (EPS), which can biosorb both Ag^+ and AgNP, acting as a permeability barrier to hinder ENP intracellular penetration, thus attenuating toxicity (Geyik and Çeçen 2016; Huangfu et al. 2019; Fig. 2). In fact, research has suggested that most ENP are effectively removed from wastewater by being embedded within the EPS-rich, porous structure of biofilms through hydrophobic interactions (Huangfu et al. 2019; Fig. 2). The level of interaction varies with the ENP coating and the biofilm surface porosity. Specifically, the hydrophobic behavior of PVP-coated AgNP led to stronger retention in EPS than the hydrophilic citrate-coated AgNP (Xiao and Wiesner 2013). The biofilm surface porosity depends on EPS properties, which in turn vary with the biosludge type (Gu et al. 2014) and the ionic strength of the medium (Huangfu et al. 2019). In addition, retention of AgNP in EPS through precipitation of Ag^+ onto EPS has also been suggested as a mechanism for ENP removal from wastewater. In fact, organosulfur compounds from EPS can play a role in the formation of sulfides, which can react with silver thiolates to produce Ag_2O (Huangfu et al. 2019). In addition, thiols can strongly interact with AgNP and influence the rates of sulfidation (Levard et al. 2012). Finally, complexation has also been proposed, as several EPS functional groups (e.g., carboxyl, hydroxyl, ether, amine and sulfhydryl groups) can act as binding sites for ENP and dissolved metal ions. Similarly, in case of endocytosis of AgNP (biological mechanism), the latter have been shown to bind to intracellular polymeric substances (IPS; Huangfu et al. 2019), such as sulfur-containing proteins and phosphorus-containing substances (e.g., DNA) and release Ag^+, which can lead to the deactivation of cellular enzymes and DNA and generation of ROS (Morones et al. 2005; Fig. 2).

3.2.3 Effect of AgNP in WWTPs

Owing to their strong antimicrobial properties, the presence of AgNP in WWTP has raised strong concerns and controversy regarding their potential adverse effects on wastewater ecosystems and biological wastewater treatment performance, potentially deteriorating contaminant removal effectiveness (Zhang et al. 2016a). In general, the ecotoxicity and extent of the negative effects of AgNP on wastewater treatment efficiency depend on several factors related to AgNP and to the treatment system (Sheng and Liu 2017; Sheng et al. 2018; Zhang et al. 2016a):

- AgNP properties (including size, shape and surface coating): larger, spherical and PVP-coated AgNP tend to have weaker bactericidal action. Generally, small AgNP can cause the severest damage on cell membranes through direct contact because of their large surface area to volume ratio and consequent high chemical activity. However, larger AgNP with a lower reactivity on the surface can persist and gradually release Ag^+ for prolonged periods in the environment, inducing potential long-term ecological hazards (Huangfu et al. 2019).
- Reaction conditions: anaerobic conditions inhibit Ag^+ release from the surfaces of AgNP and enable the steady conversion of AgNP to Ag_2S (lower solubility and toxicity), thereby minimizing the toxicity effects of AgNP on wastewater microorganisms. As a result, AgNP generally do not affect

the performance of anaerobic bioreactors (Zhang et al. 2016a).

- Presence of potential ligands in the WWTP: binding of AgNP or released Ag^+ to dissolved organic carbon and inorganic ions (namely sulfide and chloride) lower their bactericidal effects. Particularly, sulfidation has been shown to play an important role on the fate of AgNP, significantly reducing their toxicity in wastewater treatment systems by converting AgNP to Ag_2S through reaction with sulfide (Kaegi et al. 2013; Levard et al. 2012).
- Type of culture: mixed cultures are more resistant to the adverse effects of AgNP than pure cultures due to microbial functional redundancy that maintains the process stability of a wastewater treatment system (Zhang et al. 2016a). In fact, the application of high AgNP concentrations (mg L^{-1} levels or higher) can cause major shifts in the bacteria community structure without significantly affecting the reactor performance (mainly COD degradation and nitrification).
- AgNP dose and time of exposure: higher concentrations of AgNP often result in more significant adverse effects. On the other hand, the dissolution of Ag^+ from AgNP in sub-lethal concentrations has been proposed to contribute to the tolerance, resistance and stimulus-driven response of microorganisms to AgNP (Sheng and Liu 2017; Zhang et al. 2016a). Therefore, it was concluded that microbial functional redundancy and adaptability towards AgNP considerably alleviate its adverse effects on wastewater treatment performance, namely in full-scale WWTP (Zhang et al. 2016a).
- Physical structure of sludge: bacteria located on the surface of sludge flocs are more exposed to AgNP and at greater risk than the bacteria inside the flocs, which are better protected. Accordingly, microorganisms in attached-growth bioreactors (biofilm/granular sludge) are less susceptible to AgNP exposure than in suspended-growth bioreactors (flocculent sludge; Gu et al. 2014; Sheng and Liu 2011). Specifically, AgNP has been shown to alter the microbial community and the floc properties of an activated sludge sample from either a full-scale or a lab-scale suspended-growth bioreactor at relatively low silver levels (below 1 mg L^{-1}). On the other hand, the better resistance of biofilms to AgNP is generally attributed to the protective effect of the EPS matrix. Furthermore, high biofilm bacterial tolerance is often observed when AgNP (up to 200 mg L^{-1}) are added to mature biofilms, but AgNP can inhibit biofilm formation if sufficiently high concentrations are applied (Sheng and Liu 2017).
- Bacterial species: susceptibility of microorganisms to AgNP has been considered species-specific, as different wastewater microbial species/groups are differently affected by AgNP (Zhang et al. 2016a). In general, heterotrophic bacteria responsible for organic matter removal are more resistant to AgNP when compared to autotrophic bacteria, namely nitrifying bacteria (Choi et al. 2008). Specifically, it has been reported that ammonia-oxidizing bacteria (AOB) are more susceptible to inhibition by AgNP than nitrite-oxidizing bacteria (NOB) and organics-oxidizing heterotrophs (Sheng and Liu 2017; Sheng et al. 2018). Consequently, AgNP usually have stronger adverse effects on nitrification than on COD removal in wastewater treatment systems (Liang et al. 2010; Zhang et al. 2016a). Furthermore, AgNP have been shown to differently affect the phylum *Chloroflexi*, which is filamentous and possesses important functions in activated sludge, and nitrifying bacteria such as *Nitrosomonas* spp. and *Nitrosococcus* spp. (Zhang et al. 2016a).
- Treatment system/reactor configuration: transport of AgNP before the biological treatment process contributes to reducing the AgNP adverse effects by significantly decreasing their concentration and changing their chemical structure. Specifically, the sewer collection network is estimated to transform 10–95% of AgNP into silver complexes and precipitates (e.g., Ag_2S) with lower ecotoxicity (Kaegi et al. 2013; Zhang et al. 2016a). In addition, preliminary and primary treatment processes in full-scale WWTPs have been shown to partially transfer AgNP to sludge (e.g., through heteroaggregation, adsorption, settling/sedimentation), prior to the biological treatment units (King et al. 2015). For instance, approximately 35% and over 97% of the influent AgNP were removed during the mechanical processes of nine full-scale WWTP and the primary treatment in a pilot-scale WWTP, respectively (Impellitteri et al. 2013; Li et al. 2013). In contrast, only a small portion of AgNP

(approximately 10%) was removed in the sewer channel and primary clarification in a lab-scale wastewater treatment study (Hou et al. 2012; Kaegi et al. 2013). In this sense, direct addition of AgNP to lab-scale bioreactors without a sewage collection system and/or a preliminary/primary treatment process has stronger adverse effects on microorganisms and may deteriorate the reactor performance at sufficiently high concentrations (mg L^{-1} levels or higher; Zhang et al. 2016a). Zhang et al. (2016a) reviewed several studies regarding the potential effects of AgNP on the performance and microbial communities of SBRs. In general, AgNP at mg L^{-1} levels do not significantly affect wastewater microbes or long-term reactor performance of an SBR. Despite the apparently low susceptibility of SBRs to AgNP, the effect of AgNP in a continuous-flow reactor performance can be different from that exerted in an SBR, owing to the distinct physiochemical environments present (Zhang et al. 2016a).

Due to the many factors determining the ecotoxicity and detrimental effect of AgNP in wastewater treatment performance, studies have reported different consequences in biological treatment systems exposed to AgNP. For instance, Jeong et al. (2014) reported a decrease in the microbial community diversity and wastewater treatment efficiency after 50 days of AgNP supplementation. Similarly, addition of AgNP (1–5 mg L^{-1}) caused phosphorus removal deterioration and microbial community changes, subsequently stabilizing with persistent exposure to AgNP (Yuan et al. 2015). Moreover, 1 mg L^{-1} AgNP was reported to inhibit nitrification by 47% after more than 1 month of bioreactor operation (Liang et al. 2010). On the other hand, long-term (3 months) addition of 1 mg L^{-1} of spherical, PVP-coated AgNP in activated sludge bioreactors fed with a synthetic municipal wastewater was suggested to contribute to a higher microbial diversity and biomass concentration, without significantly affecting pollutant removal (COD and ammonium removal maintained above 90% and 99%, respectively; Sheng et al. 2018). In fact, recent studies focusing on long-term effects of AgNP in WWTP, indicated that although an acute inhibition by AgNP is often initially observed, the system subsequently recovers (Sheng et al. 2018). Accordingly, in the presence of minimal Ag^{+} dissolution from AgNP, the microbial community diversity and function have been maintained in activated sludge after long-term wastewater treatment (Sheng and Liu 2017). Similarly, continuous, long-term AgNP loading at low concentrations (0.1 mg L^{-1} or lower) had minimal impact on activated sludge wastewater treatment process, as the microbial community structure and abundance, as well as the effluent water quality were not affected, despite the significant increase in the copy number of a silver resistance gene (Zhang et al. 2014).

Overall, in light of the full-scale treatment system configuration, microbial functional redundancy, and microbial adaptability, Zhang et al. (2016a) argue that AgNP at environmentally realistic concentrations (μg L^{-1} or lower) do not cause significant risks to wastewater microorganisms and have minimal adverse effects of on the performance of a full-scale municipal WWTP. Yet, long-term monitoring of the AgNP toxicity in full-scale WWTP should be further investigated, as well as the long-term impacts of AgNP transformation products formed in sewage ecosystems.

3.3 Treatment of ENP-laden wastewater in AGS SBR systems

Sheng et al. (2015) showed that exposure of biofilm samples from a full-scale rotating biological contactor treating municipal sewage to high AgNP concentrations (200 mg L^{-1}) reduced the biofilm community diversity but did not significantly alter the microbial community functions. Furthermore, LB-EPS was shown to play a key role in the reported high resistance of biofilms to AgNP toxicity (Sheng and Liu 2011). In fact, sludge from attached-growth bioreactors, namely biofilm reactors, has been generally rated with higher resistance to AgNP than sludge from suspended-growth bioreactors, such as CAS bioreactors (Zhang et al. 2016a). Overall, this effect has been associated with two major aspects (Tang et al. 2018): 1) physical structure, i.e., strong bacterial cohesion and EPS provide a dense physical barrier against exposure of the biofilm inner cells to ENP; and 2) community structure, i.e., adaptation mechanisms such as proliferation of resistant individual strains, community resilience and functional redundancy are accentuated by microbial diversity and interaction within aggregates. In this context, AGS, described as a self-

supported form of biofilm, is therefore regarded as a promising solution for the treatment of AgNP-laden wastewaters, namely those produced by the textile industry. Yet, although several studies have focused on the interactions of AgNP with flocculent activated sludge (Sheng and Liu 2017; Sheng et al. 2018; Zhang et al. 2016a), reports on the fate and effect of AgNP in AGS treatment systems are rare.

Gu et al. (2014) were the first to present results on the fate and effect of AgNP in AGS systems (Table 4), comparing them with flocculent sludge systems. In general, results indicated that homoaggregation and sedimentation played an important role in removing AgNP from the liquid phase, the presence of biomass further increasing the AgNP removal through biosorption and co-sedimentation. Yet, at high concentrations, AgNP formed large aggregates and a smaller proportion of nanoparticles adsorbed to the sludge, homoaggregation being the main contributor for AgNP removal under these conditions. Specifically, flocculent sludge was more efficient in removing AgNP (30–58%) than AGS (3–9%), probably due to the former's larger specific surface area favoring adsorption. This study also showed a higher release of Ag^+ from AgNP (10 mg L^{-1}) in the presence of flocculent sludge when compared to AGS (12% vs 7% of total silver, respectively). This difference was attributed to the higher adsorption of AgNP onto flocculent sludge, leading to a better dispersion of small AgNP with higher effective surface area for Ag^+ dissolution. Conversely, the comparatively low adsorption of AgNP onto AGS probably led to a higher concentration of AgNP in the liquid, resulting in AgNP homoaggregation into larger particles, which tend to release less Ag^+ due to a lower surface area.

In terms of AgNP inhibitory effects, AGS was more resistant to AgNP toxicity than flocculent sludge, after both short- and long-term exposure (Gu et al. 2014). In fact, short-term (12 h) exposure to AgNP (1–100 mg L^{-1}) only inhibited the rate of ammonia oxidation (21–25%) in the case of flocculent sludge, indicating that nitrifying bacteria were more protected in the AG, the latter's granular structure potentially hindering the diffusion of AgNP and Ag^+ into them. On the other hand, the probably low level of toxic stress associated with exposure to low concentrations of AgNP apparently stimulated denitrification in both sludges, since denitrifying organisms are generally located in sheltered, anoxic zones (Winkler et al. 2013). Moreover, while the flocculent sludge's OUR was negatively affected by low AgNP concentrations (1 mg L^{-1}), AGS only exhibited OUR inhibition at higher AgNP levels (50–100 mg L^{-1}). However, this OUR inhibition effect in AGS was not observed after long-term exposure (22 days) to the same AgNP concentration, possibly due to adaptation mechanisms.

In contrast to the insignificant microbial activity inhibition in AGS, long-term exposure of flocculent sludge to AgNP (5 and 50 mg L^{-1}) further inhibited the rate of ammonia oxidation and OUR, in addition to negatively affecting denitrification (Gu et al. 2014). As hypothesized by the authors, the granular structure provided protection for microbes against toxic compounds not only by retarding their contact with AgNP but also due to the possible binding of EPS to dissolved Ag^+. Nevertheless, observation of cells in AG under live/dead staining suggested that AgNP or the released Ag^+ can penetrate into the core layers of AG and cause toxicity to the innermost cells. Based on the observed independent generation of ROS and release of lactate dehydrogenase (indicator of membrane permeability and integrity), the toxicity caused by AgNP was attributed to the oxidative stress induced by small AgNP (< 10 nm) and by the released Ag^+, as well as to cell membrane damage caused by both small and large (> 10 nm) AgNP, probably through physical penetration or chemical reactions.

In a subsequent study, the same research group further analyzed the long-term (69 days) effect of exposing AGS to AgNP (Quan et al. 2015; Table 4). Although high COD and NH_4-N removal yields ($> 98\%$) were maintained, the AGS microbial activity was negatively affected by the presence of AgNP from operational day 36 on, namely in terms of rate of ammonia oxidation (33%), respiration rate (18–46%) and denitrification rate (7%), in addition to a reduction in the activity of specific enzymes involved in nitrogen removal (ammonia mono-oxygenase and nitrate reductase). Similarly to that reported by Gu et al. (2014), the registered inhibition levels were independent of AgNP concentrations, probably due to the greater tendency of larger and more concentrated AgNP to aggregate, leading to reduced AgNP bioavailability or Ag^+ release from them (Quan et al. 2015).

In terms of sludge properties, SVI values gradually increased in the AGS SBR during the first month of exposure to AgNP, as compared with the AgNP-free

Table 4 Summary of operational conditions of studies on the fate and/or effect of engineered nanoparticles in aerobic granular sludge systems

System[a] (operation)	H/D;[b] V (L); VER (%)	Inoculum[c]	WW[c]	Substrate[d] (COD)	ENP;[e] size (nm)	ENP[e] (mg L^{-1})	Cycle[f]	AG size[g] (mm)	SVI^{g}_{30} (mL g^{-1})
Aerobic SBR (22 d)	16; 1.5; 50	SWW-acclim. AGS	SWW	Glucose (n.i.)	Ag; 20	1–100	Total: 4 h F: 10‘ Ae: 3.5 h S: 20′; D: 3′	850 ± 30; (n.i.)	40 (n.i.)
Aerobic SBR (69 d)	n.i.; 1.5; n.i.	SWW-acclim. AGS	SWW	Glucose (1000)	Ag; 20–70	5–50	Total: 4 h F: 10′ Ae: 3.7 h S: 1′; D: 5′	853–999 (↑)	20–40 (↑)
Anaerobic–aerobic SBR (178 d)	2.5; 1.5; 50	CAS from a municipal WWTP	Dye-laden STWW	Emsize E1 (1000)	Ag; < 100	10	Total: 6 h F: 30′ An*: 1.5 h Ae: 3.5 h S: 5′; D: 1′	n.i.	n.i.
Anaerobic/ oxic/anoxic SBR (180 d)	5; 3.6; 50	SWW-acclim. AGS	SWW	Acetate (183)	ZnO; 50–200	5–20	Total: 6 h F: 2′ An*: 2 h Ae: 1.5 h Anx*: 2.4 h S: 2′; D: 2′	n.i.	SVI_5: 21.8–23.2 (→)
Anaerobic/ oxic/anoxic SBR (n.i)	5; 3.6; 50	SWW-acclim. AGS	SWW	Acetate (150)	ZnO; 50–200	10–100	Total: 6 h F: 2′ An*: 2 h Ae: 1.5 h Anx*: 2.4 h S: 2′; D: 2′	1.5 ± 0.5 (n.i.)	SVI_5: 22.6 ± 0.7 (n.i.)

Table 4 continued

System[a] (operation)	H/D;[b] V (L); VER (%)	Inoculum[c]	WW[c]	Substrate[d] (COD)	ENP;[e] size (nm)	ENP[e] (mg L^{-1})	Cycle[f]	AG size[g] (mm)	SVI_{30}^{g} (mL g^{-1})
Anaerobic–aerobic SBR (100 d)	10; 1.4; 50	CAS from a municipal WWTP	SWW	Glucose, acetate (600)	TiO_2; < 25	10–50	Total: 4 h F: 6′ An**: 30′ Ae: 195′ S: 4′; D: 5′	0.2–1.1 (↑)	25–30 (↓)

System[a] (operation)	EPS[g]	COD removal[g] (%)	Nitrogen removal[g] (%)	Phosphorus removal[g] (%)	ENP fate	References
Aerobic SBR (22 d)	n.i.	OUR: (→ , < 50 mg AgNP L^{-1}); (↓, > 50 mg AgNP L^{-1})	AOR (→) DNR (→)	n.i.	Removed mainly by homoaggregation + sedimentation; Adsorption to AGS (500-nm Ag clusters; 3–9% at 1–8 mg AgNP L^{-1}) + co-sedimentation	Gu et al. (2014)
Aerobic SBR (69 d)	EPS (→) PN/PS (↑)	> 98 (→) OUR (↓)	> 98% (→) AOR (↓) DNR (↓)	n.i.	80–98% of total Ag removed by aggregation or adsorption (to EPS and surface if AGS) after 4-h contact	Quan et al. (2015)
Anaerobic–aerobic SBR (178 d)	n.i.	n.i.	n.i.	n.i.	AgNP clustered in agglomerates of small dimensions (< 10 μm), preferentially associated with EPS	Bento et al. (2017)
Anaerobic/oxic/anoxic SBR (180 d)	PN (↑) PS (↑) PN/PS (↑)	90–99 (↑)	TN: > 50% (↓36%) NH_4: > 60% (↓25%)	89–98% (↓)	n.i.	He et al. (2017a)
Anaerobic/oxic/anoxic SBR (n.i)	PN (↑) PS (→) PN/PS (↑)	88–97 (↑)	NH_4: 78–93 (↓) TN: 57–80 (↓) AOR (↓10–35%)	TPUR (↓ 17–38%)	n.i.	He et al. (2017b)

Table 4 continued

System[a] (operation)	EPS[g]	COD removal[g] (%)	Nitrogen removal[g] (%)	Phosphorus removal[g] (%)	ENP fate	References
Anaerobic–aerobic SBR (100 d)	PN (↑) PS (→) PN/PS (↑)	96 (→)	NH_4: > 98 (→) Nitratation (↑)	46% (→)	n.i.	Li et al. (2015)

[a]d: days; n.i.: not indicated; SBR: sequencing batch reactor

[b]H/D: height-to-diameter ratio; n.i.: not indicated; V: volume; VER: volumetric exchange ratio

[c]Acclim.: acclimatized; AGS: aerobic granular sludge; CAS: conventional activated sludge; SWW: synthetic wastewater; STWW: synthetic textile wastewater; WW: wastewater; WWTP: wastewater treatment plant

[d]COD: chemical oxygen demand (expressed as mg O_2 L^{-1}); Emsize E1: hydrolyzed hydroxypropyl starch; n.i.: not indicated

[e]Ag: silver nanoparticles; ENP: engineered nanoparticles; ZnO: zinc oxide nanoparticles; TiO_2: titanium oxide nanoparticles

[f]‘ : min; *:stirred; **: static; Ae: aerobic period; An: anaerobic period; Anx: anoxic phase; D: drain phase; F: feeding period; S: settling phase

[g]Effect of the ENP on AGS properties and treatment performance indicated in brackets: (→) remained unaffected; (↑) increased; (↓) decreased; AG: aerobic granules; AOR: ammonia oxidizing rate; DNR: denitrification rate; EPS: extracellular polymeric substances; n.i.: not indicated; NH_4: ammonia; OUR: oxygen uptake rate; PN: proteins; PS: polysaccharides; SVI_5 and SVI_{30}: sludge volume index after 5 and 30 min of settling, respectively; TN: total nitrogen; TPUR: total phosphorus uptake rate

control, the latter retaining higher biomass concentrations thereafter (Quan et al. 2015). On the other hand, long-term exposure to AgNP did not significantly affect the AG shape and size, only slightly larger dimensions (ca. 900 μm) and a looser structure than in the control AG being noted. Finally, the dominant microbial population remained stable despite slight changes in the microbial community structure, denoting the good shelter that the granular structure provides to bacteria more vulnerable to toxic environments.

In spite of the overall AGS tolerance to AgNP and absence of acute toxicity, the authors warned of a possible chronic, long-term toxicity effect resulting from the cumulative adsorption of AgNP onto AGS (Quan et al. 2015). In fact, large AgNP aggregates were found on the surface of AGS and trapped within the EPS matrix. Furthermore, AgNP were shown to accumulate in AGS along the exposure period, stimulating the preferential production of extracellular proteins (PN) over extracellular polysaccharides (PN) in EPS as a response to the toxic stress, similarly to the AgNP long-term effect observed in anammox granules (Zhang et al. 2018b). In addition, although AgNP were primarily found in major amounts in EPS, the silver content remaining in the AGS fraction after EPS extraction became more relevant at the end of the operation. These observations suggested that the continued silver influx into EPS, which served as initial barrier against AgNP and Ag^+, can eventually result in silver binding to cell membranes or penetrating into cells. Accordingly, the cell integrity in AGS was damaged and oxidative stress increased at high AgNP dosage. In addition, dead cells were found distributed from the periphery to the core of AG, the dead-to-live cells ratio being significantly higher (21–31%) than that of the AgNP-free AGS control, confirming that long-term exposure to AgNP resulted in chronic toxicity to AGS and led to cell death.

More recently, Bento et al. (2017) characterized the interaction of AgNP with AGS (Table 4) in an anaerobic–aerobic SBR treating a synthetic TWW containing the azo dye Acid Red 14 and 10 mg L^{-1} of AgNP. Nuclear microscopy analysis showed that AgNP typically clustered in agglomerates (< 10 μm) distributed throughout the biomass granules and external EPS, being preferentially associated with the latter. This observation is in accordance with the two previous studies (Gu et al. 2014; Quan et al. 2015), where the role of EPS in the capture and physical retention of AgNP was also highlighted, 500-nm clusters of silver being observed on the surface of AG (Gu et al. 2014). Furthermore, a different study reported the capacity of AGS to produce and retain palladium nanoparticles, Pd(0), through reductive precipitation of Pd(II) ions under fermentative conditions (Suja et al. 2014). This observation introduces the hypothesis of Ag^+ reduction back to Ag(0) also occurring in the EPS of AGS.

In addition to the three reviewed studies focusing on the behavior and effect of AgNP in AGS systems (Bento et al. 2017; Gu et al. 2014; Quan et al. 2015), only three reports were to date found in the literature regarding the interaction between AGS and other ENP (He et al. 2017a, b; Li et al. 2015), specifically zinc oxide and titanium oxide nanoparticles (ZnO-NP and TiO_2-NP, respectively), which are also used by the textile industry (Rezic 2011). For instance, He et al. (2017a) investigated the response of AGS to increasing concentrations of ZnO-NP along 180 days in an aerobic-oxic-anoxic SBR (Table 4). In terms of AGS properties, while settleability was not affected by the presence of ZnO-NP, the EPS content and its PN-to-PS ratio significantly increased. Moreover, exposure to ZnO-NP triggered a shift in the microbial community structure (especially at the phylum and genus levels), which became predominantly composed of *Proteobacteria* and *Bacteroidetes*. Furthermore, while the relative abundance of GAO and AOB decreased, ZnO-NP induced the accumulation of NOB, denitrifying bacteria, polyphosphate-accumulating organisms (PAO) and denitrifying PAO, the latter two being more resistant to ZnO-NP, even at high concentrations and under long-term exposure. This allowed an efficient biological phosphorus removal performance to be maintained along the experiment, in parallel with an enhanced COD removal. On the other hand, ZnO-NP led to the inhibition of both nitrification and denitrification, which is in accordance with the decreased relative abundance of AOB.

The same experimental system was further evaluated regarding the effect of ZnO-NP shock loadings on AGS (He et al. 2017b; Table 4). Similarly to the reported ZnO-NP long-term effect (He et al. 2017a), shock loading of these ENP stimulated the secretion of EPS (especially PN) and COD uptake, having no effect on the total phosphorus removal, but inhibiting nitrogen transformation (including nitrification and

denitrification). Accordingly, this study also showed that ZnO-NP significantly increased the OUR and caused acute inhibition of the rate of ammonia oxidation, but also increased phosphorus release and uptake in AGS. Overall, both studies indicated that nitrification and denitrification were more vulnerable to ZnO-NP when compared to COD and phosphorus removal (He et al. 2017a, b).

Similarly to ZnO-NP, TiO_2-NP also represent a relevant, emergent pollutant in wastewaters, namely in those generated by the textile industry (Rezic 2011). In this sense, Li et al. (2015) studied the effect of TiO_2-NP on the formation of algal–bacterial AG (Table 4). The presence of TiO_2-NP (10–50 mg L^{-1}) was shown to enhance the granulation process, stable and compact algal–bacterial granules being formed and maintained for 100 days. Conversely, in the TiO_2-NP-free SBR (control) the granulation rate was lower and AG gradually lost their structural stability after 90 days of operation (mainly due to algae overgrowth). In terms of treatment performance, the nitritration efficiency, as well as the organics and phosphorus removal yields were not affected by the presence of TiO_2-NP, which, in turn, significantly improved nitratation efficiency at concentrations above 30 mg TiO_2-NP L^{-1}. In this sense, the authors suggested that TiO_2-NP supplementation might be a strategy to prevent AG disintegration, enhancing the long-term stability of algal–bacterial granules, possibly through stimulation of EPS secretion and inhibition of filamentous overgrowth. Irrespective of the presence of TiO_2-NP, the AG microbial community was predominantly composed of *Actinobacteria*, *Bacteroidetes* (*Flavobacteria* and *Sphingobacteriia*), *Nitrospiraceae*, and *Proteobacteria* (*Alpha-*, *Beta-*, *Gamma-* and *Deltaproteobacteria*).

Overall, although some promising results have been published regarding AGS resistance towards ENP, the potential for AgNP chronic toxic effects has been highlighted. In this sense, longer operation times are required to further assess the long-term impacts of AgNP on the physical stability, biochemical properties and microbial community of AGS. Moreover, the AgNP fate, transformations and toxicity mechanisms also deserve more investigation.

4 Concluding remarks and perspectives

Textile companies typically discharge their wastewater into municipal WWTPs without proper pretreatment, because sophisticated wastewater treatment technologies are unaffordable for small to medium-sized textile companies, which constitute the majority of the textile plants. As environmental protection becomes a global concern, textile industries are looking for efficient, environmentally friendly and economically attractive TWW treatment solutions capable of diminishing their environmental impact. In this context, a biological treatment process such as the AGS technology, which allows efficient municipal wastewater treatment with a reduced footprint, lower investment and operational costs, stands out as a potential solution. Overall, this review aimed to provide relevant support for the application of the sustainable and cost-effective AGS technology in TWW treatment, specifically regarding azo dye biodegradation and removal of ENP.

The studies conducted so far on the performance and efficiency of AGS SBR systems in terms of COD and color removal from TWW constitute a valuable starting point for further studies with simulated TWW, focused on different variables relevant for the textile industry and ultimately with real TWW. Most of the studies on AGS application to the treatment of TWW operated SBRs under anaerobic and aerobic conditions, in cycles with a minimum of 6 h, for periods shorter than 200 days. Synthetic TWW containing different types of substrates, and real TWW were used with good COD removal performances, denoting AGS resistance to toxic compounds. Similarly, different types of azo dyes were tested, with color removal yields above 80% being achieved in systems employing an anaerobic reaction phase, namely when including a mechanical mixed phase for best decolorization efficiency (complete azo dye reduction achieved in a 1.5-h mixed anaerobic phase). The analysis of the azo dye breakdown products, only performed by some studies, revealed that AGS has the capacity to further degrade azo dyes, when compared to CAS, probably by favoring the establishment of a more diverse microbial population with the potential ability to biodegrade recalcitrant aromatic amines.

Overall, anaerobic–aerobic AGS SBRs have been shown as appropriate systems for stable organic load removal and decolorization of azo dye-laden textile

effluents, including the ability to further biodegrade some of the recalcitrant aromatic amines originated from azo dye reduction. In this sense, future research into the application of AGS to TWW treatment should mainly focus on: (1) optimizing anaerobic–aerobic SBR reaction conditions and hydrodynamic regimen with emphasis on granulation and decolorization; (2) optimizing reactor geometry, feeding system design and type of impellers to achieve the most effective feed distribution and mixing conditions, aiming for optimal AGS stability and cost-efficient treatment performance; (3) conducting longer operational studies to properly evaluate the long-term stability of AGS and treatment performance in anaerobic–aerobic SBRs fed with TWW; (4) evaluating the resistance of AGS to prolonged idle periods and its reactivation performance, owing to the discontinuous production processes and irregular wastewater discharges typical of the wet processing textile industry; (5) evaluating the potential aerobic biodegradation of aromatic amines, aiming to achieve dye mineralization in addition to decolorization, in order to avoid the persistence of potentially toxic dye intermediates; (6) quantifying the risk associated with the persistent metabolites by evaluating the degree of wastewater detoxification along the treatment process, in order to conduct an ecologically relevant assessment of the treatment efficiency; (7) elucidating the azo dye biodegradation pathways and involved mechanisms, which would contribute for the development of efficient TWW treatments; (8) analysing variations in the AGS SBR microbial community diversity and their correlation with specific changes in the SBR treatment performance, namely regarding the fate of aromatic amines, aiming to identify specific microbial consortia essential for aromatic amine biodegradation; (9) evaluating the capacity of AGS to deal with variable TWW compositions, namely organic and dye shock loads; (10) increasing the complexity of the wastewater by introducing other typical TWW components (e.g., other dyes, surfactants, soaps, waxes, salinity, AgNP, etc.) in order to adjust the treatment process, before eventually testing the system in the treatment of real TWW, and proceeding to scale-up.

Besides the onsite TWW treatment in textile industries, considering the co-treatment of these wastewaters with domestic sewage after a pre-treatment is also essential in view of the practical application of AGS technology for the treatment of dye-laden TWW. In this context, simultaneous biodegradation of residual textile dyes and nutrient removal (i.e., total nitrogen and total phosphorus removal) should be further studied. Although one major advantage of the AGS technology is the possibility to remove COD, nitrogen and phosphorus in a single system, the impact of azo dyes and resulting aromatic amines on nutrient removal efficiency deserves more investigation owing to their possible toxicity to key microbial groups (e.g., nitrifying bacteria), consequently compromising the nutrient removal efficiency. In addition, the potential competition between the azo dye and nutrients for reducing equivalents during the anaerobic phase could eventually decrease the decolorization or phosphorus release performances.

The increasing application of diverse ENP in different industrial fields will inevitably cause their release into industrial and municipal WWTPs, potentially affecting their biological treatment systems. Preliminary studies have shown that AGS is more resistant to AgNP toxicity than CAS, representing an advantage for the treatment of AgNP-laden wastewaters, namely those produced by the textile industry. The fate and effect of AgNP in AGS treatment systems should be further studied, namely by conducting longer experimental runs to assess a possible chronic, long-term toxicity effect on aerobic granulation, AGS stability, microbial community diversity and TWW treatment performance resulting from the cumulative adsorption of AgNP onto AGS. Moreover, although adsorption of AgNP onto AG (preferentially associated with external EPS) was shown, the fate of AgNP in the AGS system (e.g., aggregation, adsorption, dissolution, precipitation, and sulfidation) requires further investigation, namely through qualitative and quantitative analysis of silver in the biomass, EPS and treated effluent along the operation. Finally, in the context of resource recovery from wastewater, the role of EPS as recovery platform for AgNP should be assessed. In addition to AgNP, studying the impact and fate of other ENP relevant for the textile industry (e.g., TiO_2-NP) in the AGS SBR system is of utmost interest.

Acknowledgements This work was financed by Fundação para a Ciência e a Tecnologia (FCT, Portugal) through the project PTDC/AAG-TEC/4501/2014 (national funds, PIDDAC Program), the funding received by iBB – Institute for Bioengineering and Biosciences (UID/BIO/04565/2013) and

by UCIBIO – Applied Molecular Biosciences Unit (UID/Multi/04378/2019). R.D.G. Franca acknowledges the financial support from FCT (national funds, PIDDAC Program), through a doctoral grant (SFRH/BD/95415/2013).

Compliance with ethical standards

Conflict of interest The authors declare that they have no conflict of interest.

References

Adav SS, Lee D-J, Show K-Y, Tay J-H (2008) Aerobic granular sludge: recent advances. Biotechnol Adv 26:411–423. https://doi.org/10.1016/j.biotechadv.2008.05.002

Balapure K, Bhatt N, Madamwar D (2015) Mineralization of reactive azo dyes present in simulated textile waste water using down flow microaerophilic fixed film bioreactor. Bioresour Technol 175:1–7. https://doi.org/10.1016/j.biortech.2014.10.040

Barsing P, Tiwari A, Joshi T, Garg S (2011) Application of a novel bacterial consortium for mineralization of sulphonated aromatic amines. Bioresour Technol 102:765–771. https://doi.org/10.1016/j.biortech.2010.08.098

Bento JB, Franca RDG, Pinheiro T, Alves LC, Pinheiro HM, Lourenço ND (2017) Using nuclear microscopy to characterize the interaction of textile-used silver nanoparticles with a biological wastewater treatment system. Nucl Instrum Methods Phys Res B 404:150–154. https://doi.org/10.1016/j.nimb.2017.01.016

Beun JJ, Hendriks A, van Loosdrecht MCM, Morgenroth E, Wilderer PA, Heijnen JJ (1999) Aerobic granulation in a sequencing batch reactor. Water Res 33:2283–2290. https://doi.org/10.1016/S0043-1354(98)00463-1

Blaser SA, Scheringer M, MacLeod M, Hungerbühler K (2008) Estimation of cumulative aquatic exposure and risk due to silver: contribution of nano-functionalized plastics and textiles. Sci Total Environ 390:396–409. https://doi.org/10.1016/j.scitotenv.2007.10.010

Brar SK, Verma M, Tyagi RD, Surampalli RY (2010) Engineered nanoparticles in wastewater and wastewater sludge—evidence and impacts. Waste Manag 30:504–520. https://doi.org/10.1016/j.wasman.2009.10.012

Chaudhari AU, Paul D, Dhotre D, Kodam KM (2017) Effective biotransformation and detoxification of anthraquinone dye reactive blue 4 by using aerobic bacterial granules. Water Res 122:603–613. https://doi.org/10.1016/j.watres.2017.06.005

Choi O, Deng KK, Kim N-J, JrL Ross, Surampalli RY, Hua Z (2008) The inhibitory effects of silver nanoparticles, silver ions, and silver chloride colloids on microbial growth. Water Res 42:3066–3074. https://doi.org/10.1016/j.watres.2008.02.021

Çinar Ö, Yaşar S, Kertmen M, Demiröz K, Yigit NÖ, Kitis M (2008) Effect of cycle time on biodegradation of azo dye in sequencing batch reactor. Process Saf Environ Prot 86:455–460. https://doi.org/10.1016/j.psep.2008.03.001

Clara M, Kreuzinger N, Strenn B, Gans O, Kroiss H (2005) The solids retention time—a suitable design parameter to evaluate the capacity of wastewater treatment plants to remove micropollutants. Water Res 39:97–106. https://doi.org/10.1016/j.watres.2004.08.036

Collivignarelli MC, Abbà A, Miino MC, Damiania S (2019) Treatments for color removal from wastewater: state of the art. J Environ Manag 236:727–745. https://doi.org/10.1016/j.jenvman.2018.11.094

Dafale N, Wate S, Meshram S, Nandy T (2008) Kinetic study approach of remazol black-B use for the development of two-stage anoxic-oxic reactor for decolorization/biodegradation of azo dyes by activated bacterial consortium. J Hazard Mater 159:319–328. https://doi.org/10.1016/j.jhazmat.2008.02.058

Dasgupta J, Sikder J, Chakraborty S, Curcio S, Drioli E (2015) Remediation of textile effluents by membrane based treatment techniques: a state of the art review. J Environ Manag 147:55–72. https://doi.org/10.1016/j.jenvman.2014.08.008

de Kreuk MK, van Loosdrecht MCM (2004) Selection of slow growing organisms as a means for improving aerobic granular sludge stability. Water Sci Technol 49:9–17. https://doi.org/10.2166/wst.2004.0792

de Kreuk MK, Heijnen JJ, van Loosdrecht MCM (2005) Simultaneous COD, nitrogen, and phosphate removal by aerobic granular sludge. Biotechnol Bioeng 90:761–769. https://doi.org/10.1002/bit.20470

Delée W, O'Neill C, Hawkes FR, Pinheiro HM (1998) Anaerobic treatment of textile effluents: a review. J Chem Technol Biotechnol 73:323–335. https://doi.org/10.1002/(sici)1097-4660(199812)73:4%3c323:aid-jctb976%3e3.0.co;2-s

dos Santos AB, Cervantes FJ, Van Lier JB (2007) Review paper on current technologies for decoloration of textile wastewaters: perspectives for anaerobic biotechnology. Bioresour Technol 98:2369–2385. https://doi.org/10.1016/j.biortech.2006.11.013

Fabrega J, Fawcett SR, Renshaw JC, Lead JR (2009) Silver nanoparticle impact on bacterial growth: effect of pH, concentration, and organic matter. Environ Sci Technol 43:7285–7290. https://doi.org/10.1021/es803259g

Fatima M, Farooq R, Lindström RW, Saeed M (2017) A review on biocatalytic decomposition of azo dyes and electrons recovery. J Mol Liq 246:275–281. https://doi.org/10.1016/j.molliq.2017.09.063

Field JA, Stams AJM, Kato M, Schraa G (1995) Enhanced biodegradation of aromatic pollutants in cocultures of anaerobic and aerobic bacterial consortia. Antoine van Leeuwenhoek 67:47–77. https://doi.org/10.1007/BF00872195

Fitzgerald SW, Bishop PL (1995) Two stage anaerobic/aerobic treatment of sulfonated azo dyes. J Environ Sci Health A30:1251–1276. https://doi.org/10.1080/10934529509376264

Forgacs E, Cserháti T, Oros G (2004) Removal of synthetic dyes from wastewaters: a review. Environ Int 30:953–971. https://doi.org/10.1016/j.envint.2004.02.001

Forss J, Welander U (2011) Biodegradation of azo and anthraquinone dyes in continuous systems. Int Biodeterior Biodegrad 65:227–237. https://doi.org/10.1016/j.ibiod.2010.11.006

Franca RDG, Vieira A, Mata AMT, Carvalho GS, Pinheiro HM, Lourenço ND (2015) Effect of an azo dye on the performance of an aerobic granular sludge sequencing batch reactor treating a simulated textile wastewater. Water Res 85:327–336. https://doi.org/10.1016/j.watres.2015.08.043

Franca RDG, Ortigueira J, Pinheiro HM, Lourenço ND (2017) Effect of SBR feeding strategy and feed composition on the stability of aerobic granular sludge in the treatment of a simulated textile wastewater. Water Sci Technol 76:1188–1195. https://doi.org/10.2166/wst.2017.300

Franca RDG, Pinheiro HM, van Loosdrecht MCM, Lourenço ND (2018) Stability of aerobic granules during long-term bioreactor operation. Biotechnol Adv 36:228–246. https://doi.org/10.1016/j.biotechadv.2017.11.005

Gao J, Zhang Q, Su K, Chen R, Peng Y (2010a) Biosorption of Acid Yellow 17 from aqueous solution by non-living aerobic granular sludge. J Hazard Mater 174:215–225. https://doi.org/10.1016/j.jhazmat.2009.09.039

Gao JF, Zhang Q, Su K, Wang JH (2010b) Competitive biosorption of Yellow 2G and Reactive Brilliant Red K-2G onto inactive aerobic granules: simultaneous determination of two dyes by first-order derivative spectrophotometry and isotherm studies. Bioresour Technol 101:5793–5801. https://doi.org/10.1016/j.jhazmat.2009.09.039

Geyik AG, Çeçen F (2016) Exposure of activated sludge to nanosilver and silver ion: inhibitory effects and binding to the fractions of extracellular polymeric substances. Bioresour Technol 211:691–697. https://doi.org/10.1016/j.biortech.2016.03.157

Ghaly AE, Ananthashankar R, Alhattab M, Ramakrishnan VV (2014) Production, characterization and treatment of textile effluents: a critical review. J Chem Eng Process Technol 5:1–18. https://doi.org/10.4172/2157-7048.1000182

Gu L, Li Q, Quan X, Cen Y, Jiang X (2014) Comparison of nanosilver removal by flocculent and granular sludge and short- and long-term inhibition impacts. Water Res 58:62–70. https://doi.org/10.1016/j.watres.2014.03.028

Hailei W, Ping L, Guosheng L, Xin L, Jianming Y (2010) Rapid biodecolourization of eriochrome black T wastewater by bioaugmented aerobic granules cultivated through a specific method. Enzyme Microb Technol 47:37–43. https://doi.org/10.1016/j.enzmictec.2010.03.011

Haug W, Schmidt A, Nörtemann B, Hempel DC, Stolz A, Knackmuss HJ (1991) Mineralization of sulfonated azo dye Mordant Yellow 3 by a 6-aminonaphthalene-2-sulfonate-degrading bacterial consortium. Appl Environ Microbiol 57:3144–3149

He Q, Gao S, Zhang S, Zhang W, Wang H (2017a) Chronic responses of aerobic granules to zinc oxide nanoparticles in a sequencing batch reactor performing simultaneous nitrification, denitrification and phosphorus removal. Bioresour Technol 238:95–101. https://doi.org/10.1016/j.biortech.2017.04.010

He Q, Yuan Z, Zhang J, Zhang S, Zhang W, Zou Z, Wang H (2017b) Insight into the impact of ZnO nanoparticles on aerobic granular sludge under shock loading. Chemosphere 173:411–416. https://doi.org/10.1016/j.chemosphere.2017.01.085

Hisaindee S, Meetani MA, Rauf MA (2013) Application of LC-MS to the analysis of advanced oxidation process (AOP) degradation of dye products and reaction mechanisms. TrAC Trends Anal Chem 49:31–44. https://doi.org/10.1016/j.trac.2013.03.011

Holkar CR, Jadhav AJ, Pinjari DV, Mahamuni NM, Pandit AB (2016) A critical review on textile wastewater treatments: possible approaches. J Environ Manag 182:351–366. https://doi.org/10.1016/j.jenvman.2016.07.090

Hong Y, Guo J, Xu Z, Mo C, Xu M, Sun G (2007) Reduction and partial degradation mechanisms of naphthylaminesulfonic azo dye amaranth by *Shewanella* decolorationis S12. Appl Microbiol Biotechnol 75:647–654. https://doi.org/10.1007/s00253-007-0838-7

Hoque ME, Khosravi K, Newman K, Metcalfe CD (2012) Detection and characterization of silver nanoparticles in aqueous matrices using asymmetric-flow field flow fractionation with inductively coupled plasma mass spectrometry. J Chromatogr A 1233:109–115. https://doi.org/10.1016/j.chroma.2012.02.011

Hou L, Li K, Ding Y, Li Y, Chen J, Wu X, Li X (2012) Removal of silver nanoparticles in simulated wastewater treatment processes and its impact on COD and NH_4 reduction. Chemosphere 87:248–252. https://doi.org/10.1016/j.chemosphere.2011.12.042

Huang X, Wei D, Yan L, Du B, Wei Q (2018) High-efficient biosorption of dye wastewater onto aerobic granular sludge and photocatalytic regeneration of biosorbent by acid TiO_2 hydrosol. Environ Sci Pollut Res Int 25:27606–27613. https://doi.org/10.1007/s11356-018-2800-x

Huangfu X, Xu Y, Liu C, He Q, Ma J, Ma C (2019) A review on the interactions between engineered nanoparticles with extracellular and intracellular polymeric substances from wastewater treatment aggregates. Chemosphere 219:766–783. https://doi.org/10.1016/j.chemosphere.2018.12.044

Ibrahim Z, Amin MFM, Yahya A, Aris A, Muda K (2010) Characteristics of developed granules containing selected decolourising bacteria for the degradation of textile wastewater. Water Sci Technol 61:1279–1288. https://doi.org/10.2166/wst.2010.021

Impellitteri CA, Harmon S, Silva RG, Miller BW, Scheckel KG, Luxton TP, Schupp D, Panguluri S (2013) Transformation of silver nanoparticles in fresh, aged, and incinerated biosolids. Water Res 47:3878–3886. https://doi.org/10.1016/j.watres.2012.12.041

Işik M, Sponza DT (2003) Aromatic amine degradation in a UASB/CSTR sequential system treating Congo Red dye. J Environ Sci Health A Tox Hazard Subst Environ Eng 38:2301–2315. https://doi.org/10.1081/ESE-120023387

Işik M, Sponza DT (2004) Monitoring of toxicity and intermediates of C.I. Direct Black 38 azo dye through decolorization in an anaerobic/aerobic sequential reactor system. J Hazard Mater 114:29–39. https://doi.org/10.1016/j.jhazmat.2004.06.011

Işık M, Sponza DT (2004) Anaerobic/aerobic sequential treatment of a cotton textile mill wastewater. J Chem Technol Biotechnol 79:1268–1274. https://doi.org/10.1002/jctb.1122

Işık M, Sponza DT (2008) Anaerobic/aerobic treatment of a simulated textile wastewater. Sep Purif Technol 60:64–72. https://doi.org/10.1016/j.seppur.2007.07.043

Jeong E, Im W, Kim D, Kim M, Kang S, Shin H, Chae S (2014) Different susceptibilities of bacterial community to silver

nanoparticles in wastewater treatment systems. J Environ Sci Heal A 49:685–693. https://doi.org/10.1080/10934529.2014.865454

Jonstrup M, Kumar N, Murto M, Mattiasson B (2011) Sequential anaerobic-aerobic treatment of azo dyes: decolourisation and amine degradability. Desalination 280:339–346. https://doi.org/10.1016/j.desal.2011.07.022

Juárez-Ramírez C, Velázquez-García R, Ruiz-Ordaz N, Galíndez-Mayer J, Ramos MO (2012) Degradation kinetics of 4-amino naphthalene-1-sulfonic acid by a biofilm-forming bacterial consortium under carbon and nitrogen limitations. J Ind Microbiol Biotechnol 39:1169–1177. https://doi.org/10.1007/s10295-012-1123-z

Kaegi R, Voegelin A, Ort C, Sinnet B, Thalmann B, Krismer J, Hagendorfer H, Elumelu M, Mueller E (2013) Fate and transformation of silver nanoparticles in urban wastewater systems. Water Res 47:3866–3877. https://doi.org/10.1016/j.watres.2012.11.060

Kalyuzhnyi S, Sklyar V, Mosolova T, Kucherenko I, Russkova JA, Degtyaryova N (2000) Methanogenic biodegradation of aromatic amines. Water Sci Technol 42:363–370. https://doi.org/10.2166/wst.2000.0536

Kee TC, Bay HH, Lim CK, Muda K, Ibrahim Z (2014) Development of bio-granules using selected mixed culture of decolorizing bacteria for the treatment of textile wastewater. Desalin Water Treat 54:132–139. https://doi.org/10.1080/19443994.2013.877853

Khehra MS, Saini HS, Sharma DK, Chadha BS, Chimni SS (2006) Biodegradation of azo dye C.I. Acid Red 88 by an anoxic—aerobic sequential bioreactor. Dye Pigment 70:1–7. https://doi.org/10.1016/j.dyepig.2004.12.021

King SM, Jarvie H, Bowes M, Gozzard E, Lawlor A, Lawrence MJ (2015) Exploring controls on the fate of PVP-capped silver nanoparticles in primary wastewater treatment. Environ Sci Nano 2:177–190. https://doi.org/10.1039/c4en00151f

Kodam KM, Kolekar YM (2014) Bacterial degradation of textile dyes. In: Singh SN (ed) Microbial degradation of synthetic dyes in wastewaters, environmental science and engineering. Springer, Cham, pp 243–266. https://doi.org/10.1007/978-3-319-10942-8

Kolekar YM, Nemade HN, Markad VL, Adav SS, Patole MS, Kodam KM (2012) Decolorization and biodegradation of azo dye, reactive blue 59 by aerobic granules. Bioresour Technol 104:818–822. https://doi.org/10.1016/j.biortech.2011.11.046

Koupaie EH, Moghaddam MRA, Hashemi SH (2011) Post-treatment of anaerobically degraded azo dye Acid Red 18 using aerobic moving bed biofilm process: enhanced removal of aromatic amines. J Hazard Mater 195:147–154. https://doi.org/10.1016/j.jhazmat.2011.08.017

Koupaie EH, Moghaddam MRA, Hashemi SH (2013) Evaluation of integrated anaerobic/aerobic fixed-bed sequencing batch biofilm reactor for decolorization and biodegradation of azo dye Acid Red 18: comparison of using two types of packing media. Bioresour Technol 127:415–421. https://doi.org/10.1016/j.biortech.2012.10.003

Kudlich M, Bishop P, Knackmuss HJ, Stolz A (1996) Simultaneous anaerobic and aerobic degradation of the sulfonated azo dye Mordant Yellow 3 by immobilized cells from a naphthalenesulfonate-degrading mixed culture. Appl Microbiol Biotechnol 46:597–603. https://doi.org/10.1007/s002530050867

Kudlich M, Hetheridge MJ, Knackmuss HJ, Stolz A (1999) Autoxidation reactions of different aromatic o-aminohydroxynaphthalenes that are formed during the anaerobic reduction of sulfonated azo dyes. Environ Sci Technol 33:896–901. https://doi.org/10.1021/es9808346

Langford KH, Scrimshawa MD, Birkettb JW, Lestera JN (2005) Degradation of nonylphenolic surfactants in activated sludge batch tests. Water Res 39:870–876. https://doi.org/10.1016/j.watres.2004.11.033

Levard C, Hotze EM, Lowry GV, JrGE Brown (2012) Environmental transformations of silver nanoparticles: impact on stability and toxicity. Environ Sci Technol 46:6900–6914. https://doi.org/10.1021/es2037405

Li L, Hartmann G, Döblinger M, Schuster M (2013) Quantification of nanoscale silver particles removal and release from municipal wastewater treatment plants in Germany. Environ Sci Technol 47:7317–7323. https://doi.org/10.1021/es3041658

Li J, Ding LB, Cai A, Huang GX, Horn H (2014) Aerobic sludge granulation in a full-scale sequencing batch reactor. BioMed Res Int Article ID 268789, 12 p. https://doi.org/10.1155/2014/268789

Li B, Huang W, Zhang C, Feng S, Zhang Z, Lei Z, Sugiura N (2015) Effect of TiO_2 nanoparticles on aerobic granulation of algal–bacterial symbiosis system and nutrients removal from synthetic wastewater. Bioresour Technol 187:214–220. https://doi.org/10.1016/j.biortech.2015.03.118

Liang Z, Atreyee D, Zhiqiang H (2010) Bacterial response to a shock load of nanosilver in an activated sludge treatment system. Water Res 44:5432–5438. https://doi.org/10.1016/j.watres.2010.06.060

Libra JA, Borchert M, Vigelahn L, Storm T (2004) Two stage biological treatment of a diazo reactive textile dye and the fate of the dye metabolites. Chemosphere 56:167–180. https://doi.org/10.1016/j.chemosphere.2004.02.012

Liu J, Li J, Tao Y, Sellamuthu B, Walsh R (2017) Analysis of bacterial, fungal and archaeal populations from a municipal wastewater treatment plant developing an innovative aerobic granular sludge process. World J Microbiol Biotechnol 33:14–22. https://doi.org/10.1007/s11274-016-2179-0

Lotito AM, Di Iaconi C, Lotito V (2012a) Physical characterisation of the sludge produced in a sequencing batch biofilter granular reactor. Water Res 46:5316–5326. https://doi.org/10.1016/j.watres.2012.06.053

Lotito AM, Fration U, Mancini A, Bergna G, Di Iaconi C (2012b) Effective aerobic granular sludge treatment of a real dyeing textile wastewater. Int Biodeterior Biodegradation 69:62–68. https://doi.org/10.1016/j.ibiod.2012.01.004

Lotito AM, Sanctis MD, Di Iaconi C, Bergna G (2014) Textile wastewater treatment: aerobic granular sludge vs activated sludge systems. Water Res 54:337–346. https://doi.org/10.1016/j.watres.2014.01.055

Lourenço ND, Novais JM, Pinheiro HM (2000) Reactive textile dye color removal in a sequencing batch reactor. Water Sci Technol 42:321–328. https://doi.org/10.2166/wst.2000.0531

Lourenço ND, Novais JM, Pinheiro HM (2001) Effect of some operational parameters on textile dye biodegradation in a sequential batch reactor. J Biotechnol 89:163–174. https://doi.org/10.1016/S0168-1656(01)00313-3

Lourenço ND, Novais JM, Pinheiro HM (2003) Analysis of secondary metabolite fate during anaerobic-aerobic azo dye biodegradation in a sequential batch reactor. Environ Technol 24:679–686. https://doi.org/10.1080/09593330309385603

Lourenço ND, Novais JM, Pinheiro HM (2009) Treatment of colored textile wastewater in SBR with emphasis on the biodegradation of sulfonated aromatic amines. Water Pract Tech 4:1–8. https://doi.org/10.2166/wpt.2009.055

Lourenço ND, Franca RDG, Moreira MA, Gil FN, Viegas CA, Pinheiro HM (2015) Comparing aerobic granular sludge and flocculent sequencing batch reactor technologies for textile wastewater treatment. Biochem Eng J 104:57–63. https://doi.org/10.1016/j.bej.2015.04.025

Loza K, Diendorf J, Sengstock C, Ruiz-Gonzalez L, Gonzalez-Calbet JM, Vallet-Regi M, Köller M, Epple M (2014) The dissolution and biological effects of silver nanoparticles in biological media. J Mater Chem B 2:1634–1643. https://doi.org/10.1039/c3tb21569e

Ma D-Y, Wang X-H, Song C, Wang S-G, Fan M-H, Li X-M (2011) Aerobic granulation for methylene blue biodegradation in a sequencing batch reactor. Desalination 276:233–238. https://doi.org/10.1016/j.desal.2011.03.055

Manavi N, Kazemi AS, Bonakdarpour B (2017) The development of aerobic granules from conventional activated sludge under anaerobic-aerobic cycles and their adaptation for treatment of dyeing wastewater. Chem Eng J 312:375–384. https://doi.org/10.1016/j.cej.2016.11.155

Mata AMT, Pinheiro HM, Lourenço ND (2015) Effect of sequencing batch cycle strategy on the treatment of a simulated textile wastewater with aerobic granular sludge. Biochem Eng J 104:106–114. https://doi.org/10.1016/j.bej.2015.04.005

Moghaddam SS, Moghaddam MRA (2016) Aerobic granular sludge for dye biodegradation in a sequencing batch reactor with anaerobic/aerobic cycles. CLEAN Soil Air Water 44:438–443. https://doi.org/10.1002/clen.201400855

Morones JR, Elechiguerra JL, Camacho A, Holt K, Kouri JB, Ramirez JT, Yacaman MJ (2005) The bactericidal effect of silver nanoparticles. Nanotechnology 16:2346–2353. https://doi.org/10.1088/0957-4484/16/10/059

Muda K, Aris A, Salim MR, Ibrahim Z, Yahya A, Van Loosdrecht MCM, Ahmad A, Nawahwi MZ (2010) Development of granular sludge for textile wastewater treatment. Water Res 44:4341–4350. https://doi.org/10.1016/j.watres.2010.05.023

Muda K, Aris A, Salim MR, Ibrahim Z, van Loosdrecht MCM, Ahmad A, Nawahwi MZ (2011) The effect of hydraulic retention time on granular sludge biomass in treating textile wastewater. Water Res 45:4711–4721. https://doi.org/10.1016/j.watres.2011.05.012

Muda K, Aris A, Salim MR, Ibrahim Z, Yahya A (2012) Textile wastewater treatment using biogranules under intermittent anaerobic/aerobic reaction phase. JWET 10:303–315. https://doi.org/10.2965/jwet.2012.303

Nancharaiah YV, Reddy GKK (2018) Aerobic granular sludge technology: mechanisms of granulation and biotechnological applications. Bioresour Technol 247:1128–1143. https://doi.org/10.1016/j.biortech.2017.09.131

Nancharaiah YV, Sarvajith M (2019) Aerobic granular sludge process: a fast growing biological treatment for sustainable wastewater treatment. Curr Opin Environ Sci Health 12:57–65. https://doi.org/10.1016/j.coesh.2019.09.011

Nel AE, Mädler L, Velegol D, Xia T, Hoek EM, Somasundaran P, Klaessig F, Castranova V, Thompson M (2009) Understanding biophysicochemical interactions at the nano-bio interface. Nat Mater 8:543–557. https://doi.org/10.1038/nmat2442

Nimkar U (2018) Sustainable chemistry: a solution to the textile industry in a developing world. Curr Opin Green Sustain Chem 9:13–17. https://doi.org/10.1016/j.cogsc.2017.11.002

Nortemann B, Baumgarten J, Rast HG, Knackmuss HJ (1986) Bacterial communities degrading amino- and hydroxynaphthalene-2-sulfonates. Appl Environ Microbiol 52:1195–1202

O'Neill C, Lopez A, Esteves S, Hawkes FR, Hawkes DL, Wilcox S (2000) Azo-dye degradation in an anaerobic-aerobic treatment system operating on simulated textile effluent. Appl Microbiol Biotechnol 53:249–254. https://doi.org/10.1007/s002530050016

Pandey A, Singh P, Iyengar L (2007) Bacterial decolorization and degradation of azo dyes. Int Biodeterior Biodegrad 59:73–84. https://doi.org/10.1016/j.ibiod.2006.08.006

Paździor K, Klepacz-Smółka A, Ledakowicz S, Sójka-Ledakowicz J, Zyłła R (2009) Integration of nanofiltration and biological degradation of textile wastewater containing azo dye. Chemosphere 75:250–255. https://doi.org/10.1016/j.chemosphere.2008.12.016

Pearce CI, Lloyd JR, Guthrie JT (2003) The removal of colour from textile wastewater using whole bacterial cells: a review. Dyes Pigm 58:179–196. https://doi.org/10.1016/S0143-7208(03)00064-0

Pereira L, Mondal PK, Alves M (2015) Aromatic amines sources, environmental impact and remediation. In: Lichtfouse E, Schwarzbauer J, Robert D (eds) Pollutants in buildings, water and living organisms. Environmental chemistry for a sustainable world, vol 7. Springer, Cham

Peretyazhko TS, Zhang Q, Colvin VL (2014) Size-controlled dissolution of silver nanoparticles at neutral and acidic pH conditions: kinetics and size changes. Environ Sci Technol 48:11954–11961. https://doi.org/10.1021/es5023202

Pinheiro HM, Touraud E, Thomas O (2004) Aromatic amines from azo dye reduction: status review with emphasis on direct UV spectrophotometric detection in textile industry wastewaters. Dyes Pigment 61:121–139. https://doi.org/10.1016/j.dyepig.2003.10.009

Pronk M, de Kreuk MK, de Bruin B, Kamminga P, Kleerebezem R, van Loosdrecht MCM (2015) Full-scale performance of the aerobic granular sludge process for sewage treatment. Water Res 84:207–217. https://doi.org/10.1016/j.watres.2015.07.011

Quan X, Cen Y, Lu F, Gu L, Ma J (2015) Response of aerobic granular sludge to the long-term presence to nanosilver in sequencing batch reactors: reactor performance, sludge property, microbial activity and community. Sci Total

Environ 506–507:226–233. https://doi.org/10.1016/j.scitotenv.2014.11.015
Radetić M (2013) Functionalization of textile materials with silver nanoparticles. J Mater Sci 48:95–107. https://doi.org/10.1007/s10853-012-6677-7
Raman CD, Kanmani S (2016) Textile dye degradation using nano zero valent iron: a review. J Environ Manag 177:341–355. https://doi.org/10.1016/j.jenvman.2016.04.034
Rangabhashiyam S, Anu N, Selvaraju N (2013) Sequestration of dye from textile industry wastewater using agricultural waste products as adsorbents. J Environ Chem Eng 1:629–641. https://doi.org/10.1016/j.jece.2013.07.014
Rawat D, Mishra V, Sharma RS (2016) Detoxification of azo dyes in the context of environmental processes. Chemosphere 155:591–605. https://doi.org/10.1016/j.chemosphere.2016.04.068
Razo-Flores E, Luijten M, Donlon B, Lettinga G, Field J (1997) Biodegradation of selected azo dyes under methanogenic conditions. Water Sci Technol 36:65–72. https://doi.org/10.1016/S0273-1223(97)00508-8
Rezić I (2011) Determination of engineered nanoparticles on textiles and in textile wastewaters. Trends Anal Chem 30:1159–1167. https://doi.org/10.1016/j.trac.2011.02.017
Rollemberg SLS, Barros ARM, Milen Firmino PI, dos Santos AB (2018) Aerobic granular sludge: cultivation parameters and removal mechanisms. Bioresour Technol 270:678–688. https://doi.org/10.1016/j.biortech.2018.08.130
Saratale RG, Saratale GD, Chang JS, Govindwar SP (2011) Bacterial decolorization and degradation of azo dyes: a review. J Taiwan Inst Chem Eng 42:138–157. https://doi.org/10.1016/j.ibiod.2006.08.006
Sarayu K, Sandhya S (2012) Current technologies for biological treatment of textile wastewater—a review. Appl Biochem Biotechnol 167:645–661. https://doi.org/10.1007/s12010-012-9716-6
Sarvajith M, Reddy GKK, Nancharaiah Y (2018) Textile dye biodecolourization and ammonium removal over nitrite in aerobic granular sludge sequencing batch reactors. J Hazard Mater 342:536–543. https://doi.org/10.1016/j.jhazmat.2017.08.064
Sen SK, Raut S, Bandyopadhyaya P, Raut S (2016) Fungal decolouration and degradation of azo dyes: a review. Fungal Biol Rev 30:112–133. https://doi.org/10.1016/j.fbr.2016.06.003
Shaw CB, Carliell CM, Wheatley AD (2002) Anaerobic/aerobic treatment of coloured textile effluents using sequencing batch reactors. Water Res 36:1993–2001. https://doi.org/10.1016/S0043-1354(01)00392-X
Sheng Z, Liu Y (2011) Effects of silver nanoparticles on wastewater biofilms. Water Res 45:6039–6050. https://doi.org/10.1016/j.watres.2011.08.065
Sheng ZY, Liu Y (2017) Potential impacts of silver nanoparticles on bacteria in the aquatic environment. J Environ Manag 191:290–296. https://doi.org/10.1016/j.jenvman.2017.01.028
Sheng Z, Van Nostrand JD, Zhou J, Liu Y (2015) The effects of silver nanoparticles on intact wastewater biofilms. Front Microbiol 6, Article 680. https://doi.org/10.1016/j.watres.2011.08.065
Sheng ZW, Nostrand JDV, Zhou JZ, Liu Y (2018) Contradictory effects of silver nanoparticles on activated sludge wastewater treatment. J Hazard Mater 341:448–456. https://doi.org/10.1016/j.jhazmat.2017.07.051
Singh RL, Singh PK, Singh RP (2015) Enzymatic decolorization and degradation of azo dyes—a review. Int Biodeterior Biodegradation 104:21–31. https://doi.org/10.1016/j.ibiod.2015.04.027
Solís M, Solís A, Pérez HI, Manjarrez N, Flores M (2012) Microbial decolouration of azo dyes: a review. Process Biochem 47:1723–1748. https://doi.org/10.1016/j.procbio.2012.08.014
Spagni A, Grilli S, Casu S, Mattioli D (2010) Treatment of a simulated textile wastewater containing the azo-dye reactive orange 16 in an anaerobic-biofilm anoxic-aerobic membrane bioreactor. Int Biodeterior Biodegrad 64:676–681. https://doi.org/10.1016/j.ibiod.2010.08.004
Sponza DT, Işik M (2005) Toxicity and intermediates of C.I. Direct Red 28 dye through sequential anaerobic/aerobic treatment. Process Biochem 40:2735–2744. https://doi.org/10.1016/j.procbio.2004.12.016
Sponza DT, Işık M (2002) Decolorization and azo dye degradation by anaerobic/aerobic sequential process. Enzyme Microb Technol 31:102–110. https://doi.org/10.1016/S0141-0229(02)00081-9
Sponza DT, Işık M (2005) Reactor performances and fate of aromatic amines through decolorization of Direct Black 38 dye under anaerobic/aerobic sequentials. Process Biochem 40:35–44. https://doi.org/10.1016/j.procbio.2003.11.030
Stolz A (2001) Basic and applied aspects in the microbial degradation of azo dyes. Appl Microbiol Biotechnol 56:69–80. https://doi.org/10.1007/s002530100686
Stolz A, Knackmuss HJ (1993) Bacterial metabolism of 5-aminosalicylic acid enzymic conversion to L-malate, pyruvate and ammonia. J Gen Microbiol 139:1019–1025. https://doi.org/10.1099/00221287-139-5-1019
Suja E, Nancharaiah YV, Venugopalan VP (2014) Biogenic nanopalladium production by self-immobilized granular biomass: application for contaminant remediation. Water Res 65:395–401. https://doi.org/10.1016/j.watres.2014.08.005
Tan NCG, Lettinga G, Field JA (1999a) Reduction of the azo dye Mordant Orange 1 by methanogenic granular sludge exposed to oxygen. Bioresour Technol 67:35–42. https://doi.org/10.1016/S0960-8524(99)00098-X
Tan NCG, Prenafeta-Boldú FX, Opsteeg JL, Lettinga G, Field JA (1999b) Biodegradation of azo dyes in cocultures of anaerobic granular sludge with aerobic aromatic amine degrading enrichment cultures. Appl Microbiol Biotechnol 51:865–871. https://doi.org/10.1007/s002530051475
Tan NCG, Slenders P, Svitelskaya A, Lettinga G, Field JA (2000) Degradation of azo dye Mordant Yellow 10 in a sequential anaerobic and bioaugmented aerobic bioreactor. Water Sci Technol 42:337–344. https://doi.org/10.2166/wst.2000.0533
Tan NCG, Van Leeuwen A, Van Voorthuizen EM, Slenders P, Prenafeta-Boldú FX, Temmink H, Lettinga G, Field JA (2005) Fate and biodegradability of sulfonated aromatic amines. Biodegradation 16:527–537. https://doi.org/10.1007/s10532-004-6593-x

Tang J, Wu Y, Esquivel-Elizondo S, Sørensen SJ, Rittmann BE (2018) How microbial aggregates protect against nanoparticle toxicity. Trends Biotechnol 36:1171–1182. https://doi.org/10.1016/j.tibtech.2018.06.009

Vajnhandl S, Valh JV (2014) The status of water reuse in European textile sector. J Environ Manag 141:29–35. https://doi.org/10.1016/j.jenvman.2014.03.014

van der Zee FP, Villaverde S (2005) Combined anaerobic-aerobic treatment of azo dyes—a short review of bioreactor studies. Water Res 39:1425–1440. https://doi.org/10.1016/j.watres.2005.03.007

Verma AK, Dash RR, Bhunia P (2012) A review on chemical coagulation/flocculation technologies for removal of colour from textile wastewaters. J Environ Manag 93:154–168. https://doi.org/10.1016/j.jenvman.2011.09.012

Wei D, Wang BF, Ngo HH, Guo WS, Han F, Wang XD, Du B, Wei Q (2015) Role of extracellular polymeric substances in biosorption of dye wastewater using aerobic granular sludge. Bioresour Technol 185:14–20. https://doi.org/10.1016/j.biortech.2015.02.084

Windler L, Height M, Nowack B (2013) Comparative evaluation of antimicrobials for textile applications. Environ Int 53:62–73. https://doi.org/10.1016/j.envint.2012.12.010

Winkler M-KH, Kleerebezem R, de Bruin LMM, Verheijen PJT, Abbas B, Habermacher J, van Loosdrecht MCM (2013) Microbial diversity differences within aerobic granular sludge and activated sludge flocs. Appl Microbiol Biotechnol 97:7447–7458. https://doi.org/10.1007/s00253-012-4472-7

Xia J, Ye L, Ren H, Zhang X-X (2018) Microbial community structure and function in aerobic granular sludge. Appl Microbiol Biotechnol 102:3967–3979. https://doi.org/10.1007/s00253-018-8905-9

Xiao Y, Wiesner MR (2013) Transport and retention of selected engineered nanoparticles by porous media in the presence of a biofilm. Environ Sci Technol 47:2246–2253. https://doi.org/10.1021/es304501n

You SJ, Teng JY (2009) Performance and dye-degrading bacteria isolation of a hybrid membrane process. J Hazard Mater 172:172–179. https://doi.org/10.1016/j.jhazmat.2009.06.149

Yu S, Yin Y, Zhou X, Dong L, Liu J (2016) Transformation kinetics of silver nanoparticles and silver ions in aquatic environments revealed by double stable isotope labeling. Environ Sci Nano 3:883–893. https://doi.org/10.1039/c6en00104a

Yuan Z, Yang X, Hu A, Yu C (2015) Long-term impacts of silver nanoparticles in an anaerobic-anoxic-oxic membrane bioreactor system. Chem Eng J 276:83–90. https://doi.org/10.1016/j.cej.2015.04.059

Zhang C, Liang Z, Hu Z (2014) Bacterial response to a continuous long-term exposure of silver nanoparticles at sub-ppm silver concentrations in a membrane bioreactor activated sludge system. Water Res 50:350–358. https://doi.org/10.1016/j.watres.2013.10.047

Zhang C, Hu Z, Li P, Gajaraj S (2016a) Governing factors affecting the impacts of silver nanoparticles on wastewater treatment. Sci Total Environ 572:852–873. https://doi.org/10.1016/j.scitotenv.2016.07.145

Zhang Y, Li J, Li W, Chen G (2016b) Utilization of inactivated aerobic granular sludge as a potential adsorbent for the removal of sunset yellow FCF. Desalin Water Treat 57:7334–7344. https://doi.org/10.1080/19443994.2015.1019372

Zhang W, Xiao B, Fang T (2018a) Chemical transformation of silver nanoparticles in aquatic environments: mechanism, morphology and toxicity. Chemosphere 191:324–334. https://doi.org/10.1016/j.chemosphere.2017.10.016

Zhang ZZ, Cheng YF, Xu LZJ, Bai YH, Jin RC (2018b) Anammox granules show strong resistance to engineered silver nanoparticles during long-term exposure. Bioresour Technol 259:10–17. https://doi.org/10.1016/j.biortech.2018.03.024

Zheng YM, Yu HQ, Sheng GP (2005) Physical and chemical characteristics of granular activated sludge from a sequencing batch airlift reactor. Process Biochem 40:645–650. https://doi.org/10.1016/j.procbio.2004.01.056